AFOSR-TR- 82-0659

(5)

S-CUBED
FORMERLY
Systems, Science and Software

SSS-R-82-5481
W/O 11127

SIMULATION OF REGIONAL SEISMIC PHASES

H. J. Swanger

FINAL TECHNICAL REPORT

Sponsored by

Advanced Research Projects Agency
ARPA Order No. 3291-32

March 1982

P. O. Box 1620
La Jolla, California
92038
(714)453-0060

ARPA Order No. 3291-32, Program Code No. 0D60
Contractor: Systems, Science and Software
Effective Date of Contract: 1 October 1979
Contract Expiration Date: 30 September 1980
Amount of Contract: $88,024
Contract No: F49620-80-C-0019
Principal Investigator and Phone No:
Dr. Thomas C. Bache, (714) 453-0060, Ext. 337
Program Manager and Phone No:
Dr. Thomas C. Bache, (714) 453-0060, Ext. 337
Title: Theoretical Basis for Regional Discrimination

This research was supported by the Advanced Research Projects Agency of the Department of Defense and was monitored by the Air Force Office of Scientific Research under Contract No. F49620-80-C-0019.

W/O 11127

Unclassified

SECURITY CLASSIFICATION OF THIS PAGE (When Data Entered)

REPORT DOCUMENTATION PAGE	READ INSTRUCTIONS BEFORE COMPLETING FORM
1. REPORT NUMBER: AFOSR-TR- 82-0659	2. GOVT ACCESSION NO.: AD-A118952
3. RECIPIENT'S CATALOG NUMBER	
4. TITLE (and Subtitle): Simulation of Regional Seismic Phases	5. TYPE OF REPORT & PERIOD COVERED: Final Technical Report June 1, 1981-Nov. 30, 1981
6. PERFORMING ORG. REPORT NUMBER: SSS-R-82-5481	
7. AUTHOR(s): H. J. Swanger	8. CONTRACT OR GRANT NUMBER(s): F49620-80-C-0019
9. PERFORMING ORGANIZATION NAME AND ADDRESS: Systems, Science and Software, P.O. Box 1620, La Jolla, California 92038	10. PROGRAM ELEMENT, PROJECT, TASK AREA & WORK UNIT NUMBERS: ARPA Order No. 3291-32, 62714E 2309/A1
11. CONTROLLING OFFICE NAME AND ADDRESS: Air Force Office of Scientific Research, Bolling Air Force Base, Washington, D.C. 20322	12. REPORT DATE: March 1982
	13. NUMBER OF PAGES: 63
14. MONITORING AGENCY NAME & ADDRESS (if different from Controlling Office)	15. SECURITY CLASS. (of this report): Unclassified
	15a. DECLASSIFICATION DOWNGRADING SCHEDULE

16. DISTRIBUTION STATEMENT (of this Report)

Approved for public release; distribution unlimited.

17. DISTRIBUTION STATEMENT (of the abstract entered in Block 20, if different from Report)

18. SUPPLEMENTARY NOTES

19. KEY WORDS (Continue on reverse side if necessary and identify by block number)

Lg
Synthetic seismograms
Seismic phases
Codas

20. ABSTRACT (Continue on reverse side if necessary and identify by block number)

This report summarizes efforts to simulate the characteristics of regional seismic phases from earthquakes and explosions. The objective is to use computer generated seismograms to aid our understanding of the origin of regional phases and to examine possible discriminants in regional recordings from earthquakes and explosions. This involves four distinct studies. First, the source-depth dependence of the phase Lg is examined. It is found that the depth dependence of synthetic Lg for double-couple sources can be explained by changes

(continued)

DD FORM 1 JAN 73 1473 EDITION OF 1 NOV 65 IS OBSOLETE

Unclassified

SECURITY CLASSIFICATION OF THIS PAGE (When Data Entered)

20. ABSTRACT: (continued)

in material properties over crustal depths combined with radiation pattern effects for S-waves radiated with the phase velocities appropriate to Lg. It was found that one particular double-couple orientation is very anomalous in its Lg exitation and is probably not representative of a typical earthquake source.

The second effort reported is a study of Lg propagation in the Basin and Range tectonic province. For the Basin and Range, most of the energy is trapped above an intermediate crustal reflector, whereas eastern United States and Eurasian crustal structures Lg was found to be a guided wave between the earth's surface and the Moho. This suggests that the characteristics of Lg propagation in the Basin and Range may be different from that in other crustal structures, and the observations made in that environment may not be appropriate to other tectonic provinces.

Third, we examine two observations made concerning differences in the characteristics of Lg radiated from earthquakes and explosions. Rondout Associates observed more late arriving energy relative to early arriving energy from the explosion SALMON than from earthquakes in eastern United States. Synthetic seismograms for eastern United States crustal structure also show this feature, but it is found not to be a source-depth effect. We also investigated observed spectral differences in Lg spectra for explosions and earthquakes from the area of NTS. Synthetic Lg spectra cannot conclusively support the observations in this case.

Finally, we investigated the behavior of Lg codas as they are transmitted across boundaries between two different crustal structures. It is found that a large change in crustal thickness, which has been suggested as a reason Lg is not prominent in some tectonic provinces, is not sufficient to explain a disappearance of Lg.

TABLE OF CONTENTS

LIST OF ILLUSTRATIONS

TABLE OF CONTENTS (Continued)

LIST OF TABLES

I. INTRODUCTION

This report summarizes efforts to simulate the characteristics of regional seismic phases from earthquakes and explosions and to modify existing three-dimensional finite difference codes for use on the Cray-1 computer. The objective of the regional phase task is to use computer generated seismograms to aid our understanding of the origin of regional phases and to examine possible discriminants in regional recordings from earthquakes and explosions. The objective of the finite-difference code conversion effort is to extend existing capabilities for simulating earthquake faulting in realistic geologies.

The computational studies of regional seismic phases include four distinct studies. First, the source-depth dependence of the phase Lg is examined in Section II. This is a followup to work reported by Bache, et al. (1981). It is found that the depth dependence of synthetic Lg for double-couple sources can be explained by changes in material properties over crustal depths combined with radiation pattern effects for S-waves radiated with the phase velocities appropriate to Lg. It was found that one of the double-couple orientations considered by Bache, et al. (1981) is very anomalous in its Lg excitation and is probably not representative of a typical earthquake source.

The second effort reported is a study of Lg propagation in the Basin and Range tectonic province, and this is summarized in Section III. It is shown that the mechanism of Lg propagation in this environment is different from that of other crustal environments, such as those examined by Bache, et al. (1980, 1981). For eastern United States and Eurasian crustal structures, Lg was found to be a guided wave between the earth's surface and the Moho. For the Basin and Range, most of the energy is trapped above an intermediate crustal reflector. This suggests that the characteristics of Lg propagation in the Basin and Range may be different from that in other crustal structures, and the observations made in that environment may not be appropriate to other tectonic provinces.

In Section IV we examine two observations made concerning differences in the characteristics of Lg radiated from earthquakes and explosions. Rondout Associates (1980) observed more late arriving energy relative to early arriving energy from the explosion SALMON than from earthquakes in eastern United States. Synthetic seismograms for eastern United States crustal structure also show this feature, but it is found not to be a source-depth effect. We also investigated an observation by Murphy, et al. (1981) who observed spectral differences in Lg spectra for explosions and earthquakes from the area of NTS. Synthetic Lg spectra cannot conclusively support the observations in this case.

In Section V we employed the method of Alsop (1966) to investigate the behavior of Lg codas as they are transmitted across boundaries between two different crustal structures. It is found that a large change in crustal thickness, which has been suggested as a reason Lg is not prominent in some tectonic provinces, is not sufficient to explain a disappearance of Lg.

II. A CLOSER EXAMINATION OF THE THEORETICAL DEPTH DEPENDENCE OF Lg

2.1 INTRODUCTION

In a previous report (Bache, et al., 1981), the source-depth dependence of Lg, for dislocation sources, was examined using synthetic seismograms. In that study the theoretical depth dependence of Lg amplitudes was found to depend strongly on focal mechanism. Three fundamental focal mechanisms were considered-vertical dip-slip, vertical strike-slip, and 45 degree oblique thrust events. The vertical strike-slip and the oblique thrust event gave very similar depth dependences, while the vertical dip-slip event was considerably different. This imples that Lg amplitudes should be used with caution for discrimination purposes. For example, discriminants based on Lg amplitudes found for a specific type of source mechanism in a certain tectonic environment may not be applicable in a different tectonic environment where different earthquake focal mechanisms are common.

Here we attempt to find an explanation for this phenomenon. We will show that the depth dependence of Lg computed with multi-mode Rayleigh waves is very similar to the depth dependence expected for SV-waves radiated at takeoff angles with phase velocities like those of Lg. Almost all the characteristics observed in the Lg amplitudes as a function of depth for dislocation sources can be explained simply by the double-couple radiation pattern and by the material properties at the source-depth. A closer examination of the radiation pattern of SV-waves with the phase velocities in the range of interest shows that the focal mechanism giving anomalous amplitudes (vertical dip-slip) found in the calculations of Bache, et al. (1981) is very anamolous with respect to all other focal mechanisms common to earthquakes. Examination of theoretical SV-wave radiation for a wide variety of focal mechanisms suggests that the average trend in source-depth dependence is approximately that found for a vertical strike-slip source or an oblique thrust. We conclude that on the average, the amplitudes of Lg as a function

of source-depth should scale much the same as teleseismic P-waves except for very shallow depth earthquakes.

2.2 REVIEW OF PAST WORK

Bache, et al. (1981) considered the depth dependence of Lg from dislocation sources in the eastern United States crustal model given in Table 1. The theoretical Lg phases were computed for point dislocation sources at various depths with a step-dislocation time history. The response was filtered by a short-period LRSM instrument at a range of 1000 kilometers. The amplitudes used for comparison were the largest amplitudes sustained over three successive cycles during the first ten seconds of the Lg coda.

Figure 1 shows the depth dependence found for Lg as a function of depth for three focal mechanisms for fixed m_b in an eastern United States crustal structure. Bache, et al. also considered the dependence as a function of depth for fixed moment. Relations between fixed moment and fixed m_b are given in Bache, et al. (1981). For vertical strike-slip and 45 degree thrust mechanisms, the amplitudes of Lg with depth are relatively constant with respect to fixed m_b except at very shallow depths and below about 20 kilometers. The vertical dip-slip mechanism, on the other hand, shows a very noticeable dependence. The amplitudes increase with increasing source-depth. The response to a dislocation of any orientation can be determined from a linear combination of these three focal mechanisms. We might expect then, that the trend for vertical dip-slip sources should appear in many different kinds of focal mechanisms. This would suggest that the depth dependence for Lg should be highly focal mechanism dependent.

No explanation for this observation was given in Bache, et al. (1981). Here we will consider the possibility of a radiation pattern effect being the cause of this dependence. From the modal studies of Bache, et al., we know the range of phase velocities which contribute to the Lg coda. We can use these phase velocities and return to the source and interpret Lg in terms of SV-waves and

TABLE 1

CENTRAL AND EASTERN UNITED STATES CRUSTAL MODELS

Layer	Depth (km)	Thickness (km)	α (km/sec)	β (km/sec)	ρ (gm/cm^3)	Q
			(Model S1 Bache, Swanger and Shkoller, 1980)			
1	0.6	0.6	3.70	2.16	2.10	20
2	2.6	2.0	4.55	2.54	2.20	50
3	4.1	1.5	5.60	3.14	2.65	250
4	6.2	2.1	6.10	3.30	2.85	400
5	13.2	7.0	6.30	3.41	2.94	1200
6	19.0	5.8	6.40	3.46	3.00	1500
7	34.0	15.0	6.60	3.59	3.05	2000
8	0.0	0.0	8.10	4.52	3.35	2000

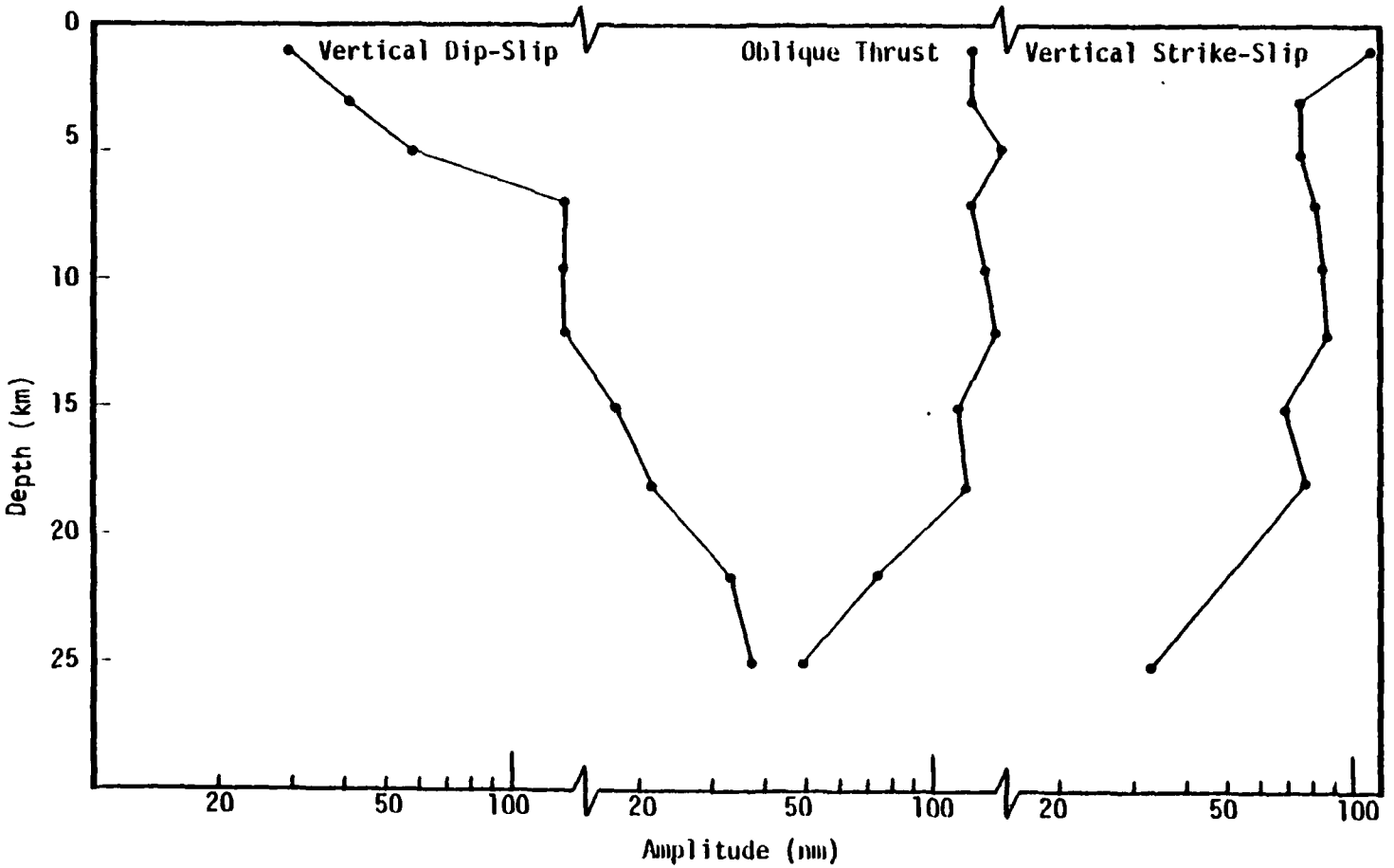

Figure 1. Lg amplitudes as a function of source depth for fixed "m_b" at 1000 km in an EUS crustal model (from Bache, et al., 1981).

P-waves radiating from the source at takeoff angles appropriate to these phase velocities. For dislocation sources, we would expect a dominant contributor to Lg to be the SV-waves, considering tnat there is five times more energy in the shear waves radiating from a dislocation than in the compressional waves. In the next section we consider tne radiation pattern of SV-waves from dislocation sources with takeoff angles in the range of interest to Lg.

2.3 SV-WAVE RADIATION PATTERN FOR Lg PHASE VELOCITIES

A radiation pattern of SV-waves for various focal mechanisms as a function of angle of incidence can be found in many places. Aki and Richards (1981), for example, express the SV-radiation pattern as

$$
\begin{aligned}
F^{SV} &= [(\gamma \cdot \nu)(\dot{\bar{u}} \cdot \hat{p}) + (\gamma \cdot \dot{\bar{u}})(\nu \cdot \hat{p})]/\dot{\bar{u}} \\
&= \sin\lambda \cos 2\delta \cos 2i\xi \sin(\phi - \phi_s) - \\
&\quad \cos\lambda \cos\delta \cos 2i\xi \cos(\phi - \phi_s) \\
&\quad + \tfrac{1}{2} \cos\lambda \sin\delta \sin 2i\xi \sin 2(\phi - \phi_s) \\
&\quad - \tfrac{1}{2} \sin\lambda \sin 2\delta \sin 2i\xi (1 + \sin^2(\phi - \phi_s)),
\end{aligned}
\tag{1}
$$

where

- δ = fault dip
- λ = fault slip angle
- θ_s = fault strike
- ϕ = receiver azimuth
- $i\xi$ = takeoff angle from the vertical

The SV-radiation pattern as a function of takeoff angle for vertical strike-slip and vertical dip-slip sources is shown graphically in Figure 2. Here we have taken cross-sections of the radiation patterns for these two focal mechanisms. Note that for a vertical strike-slip source we have nodes for SV-waves with

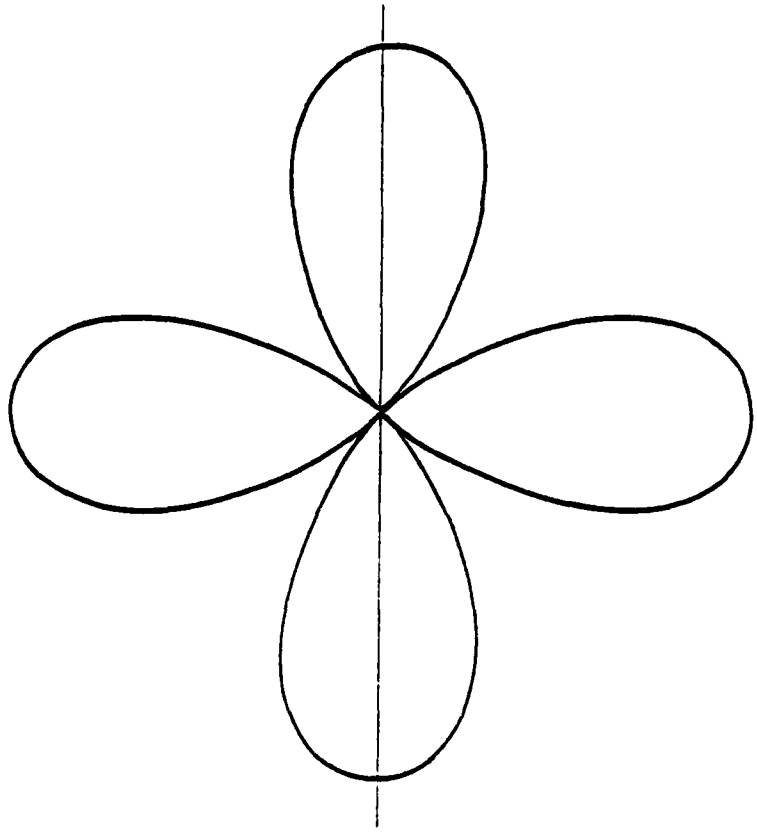

Vertical Dip-Slip

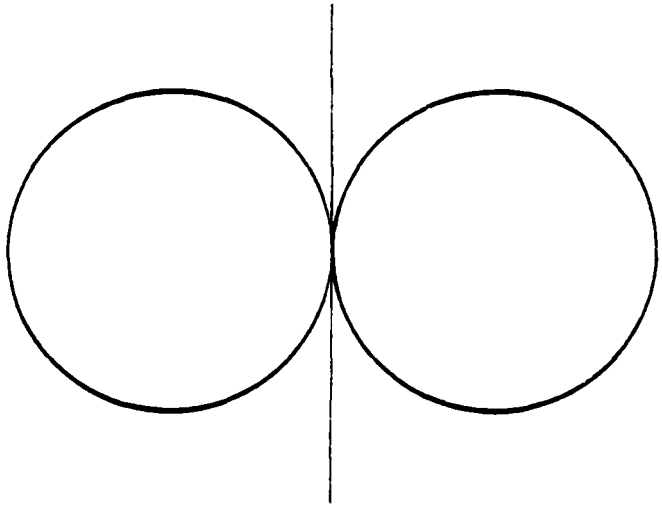

Vertical Strike-Slip

Figure 2. Vertical cross-sections of the SV-wave radiation pattern for vertical strike-slip and vertical dip-slip double couples.

horizontal and vertical takeoff angles, and an antinode at 45 degrees. In this case, we should expect the radiation pattern to be relatively constant except for near horizontal or near vertical takeoff angles. The vertical dip-slip, on the other hand, has a maximum for horizontal takeoff angles and nodes for vertical takeoff angles. We would expect significant difference between the energy radiated for shallow takeoff angles and steep takeoff angles.

From the dispersion characteristics of the eastern United States structure used by Bache, et al. (1981), we have estimated the phase velocity range of Lg to be 3.6 to 4.0 kilometers per second. At shallow depths, where the shear velocity is considerably less than this range, SV-waves in this phase velocity range will have rather steep takeoff angles. For sources at the base of the crust, SV-waves in this phase velocity window have nearly horizontal takeoff. We should expect that the radiation pattern for vertical dip-slip source should be rather weak for shallow sources and much stronger for a well buried source. We would expect the largest amplitude for the vertical dip-slip source to occur when the dislocation is located just above the Moho. For vertical strike-sources on the other hand, we would expect the amplitudes to be relatively constant except if the waves are actually traveling nearly vertical, which would be the case for a source located in materials with a very slow shear velocity.

Radiation patterns for SV-waves for the three focal mechanisms considered earlier were computed from formulas of Aki and Richards, averaged overall azimuths. Figure 3 shows the depth dependence found for the three source orientations for a particular phase velocity in the Lg range. The depth dependence for fixed m_b is shown to be quite similar to the depth dependence found for Lg earlier. We can infer then that the trends seen in Figure 1 are due to SV-wave radiation pattern effects.

Next we will examine the theoretical SV-wave radiation patterns for a wide range of focal mechanisms. In the synthetic seismogram studies we considered only three mechanisms. Here, by

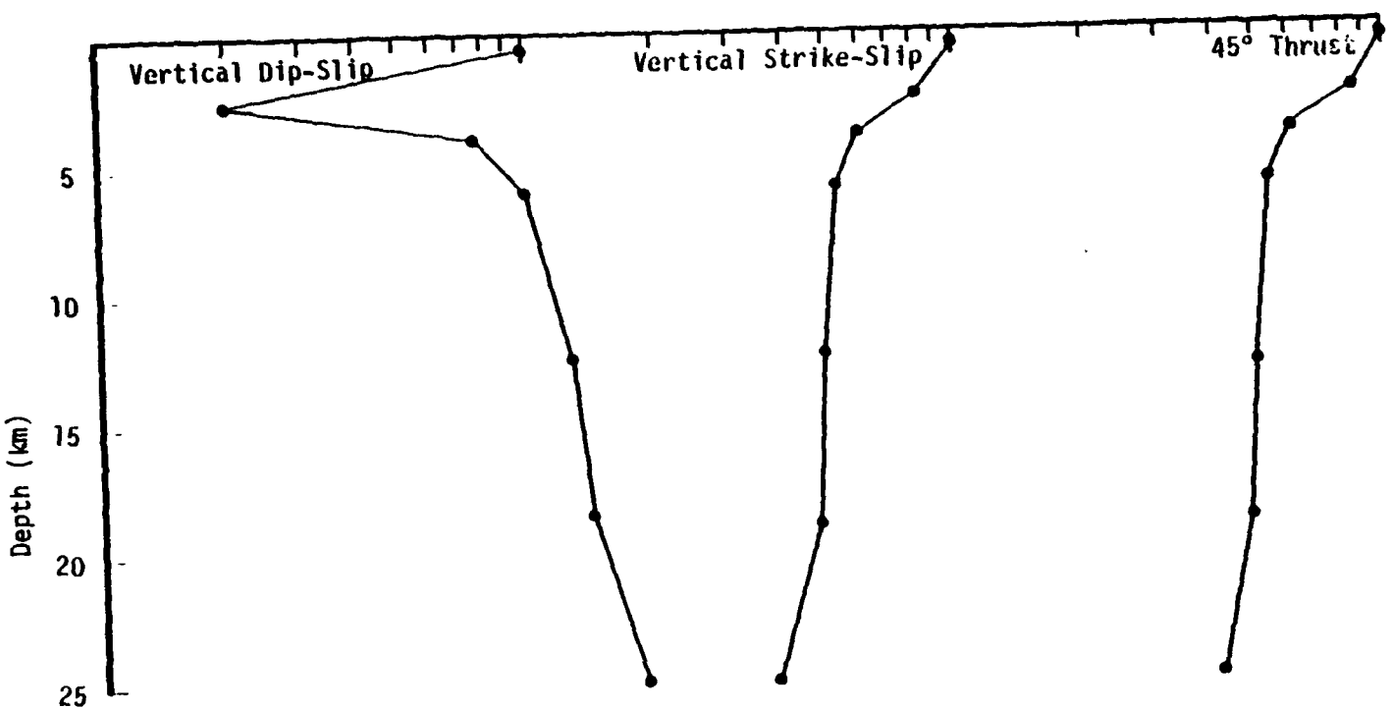

Figure 3. Radiation pattern as a function of depth for SV-waves with phase velocity of 3.75 km/sec in EUS crustal model. Amplitudes normalized to unity at 0.5 km depth.

using radiation patterns, we can look at a suite of mechanisms to determine how typical the three mechanisms considered earlier are with respect to all possible earthquake focal mechanisms. We will consider all slip angles and fault dips ranging from 30 to 90 degrees. In Figure 4 we show the average amplitude and standard deviations of the SV-wave amplitude as a function of depth for fixed phase velocity for 2000 randomly oriented dislocations. Note that, on the average, the type of depth dependence seen for a vertical strike-slip source and a 45 degree thrust source is much more common than that observed for a vertical dip-slip source. We might consider the vertical dip-slip source as anomalous with respect to all possible focal mechanisms, and we should possibly disregard this anamolous behavior in determining expected trends of the depth dependence of dislocations in Lg amplitudes. Vertical dip-slip sources are not very common in nature, and it is difficult to imagine tectonic processes which could cause a stress field which would result in a vertical dip-slip event.

2.4 SUMMARY

We have examined more closely the computed amplitudes as a function of source-depth of Lg eastern United States crustal structure. We have assumed that Lg consists of waves in a narrow range of phase velocities. We have examined the amplitude dependence of SV-waves for this range of phase velocities and found that the radiation pattern effect coming from the change in takeoff angle as a function of source-depth can explain much of the depth dependence seen in theoretical Lg. From the calculations of Bache, et al. (1981), it would appear that the depth dependence of Lg amplitude is highly focal mechanism dependent, and that we would have to consider a wide range of possibilities in terms of using depth dependent amplitude characteristics for discrimination purposes. Here we have shown, by examining the SV-wave radiation patterns from a number of focal mechanisms, that one of the mechanisms considered by Bache, et al., namely the vertical dip-slip source is highly anomalous, and the depth dependence as found for

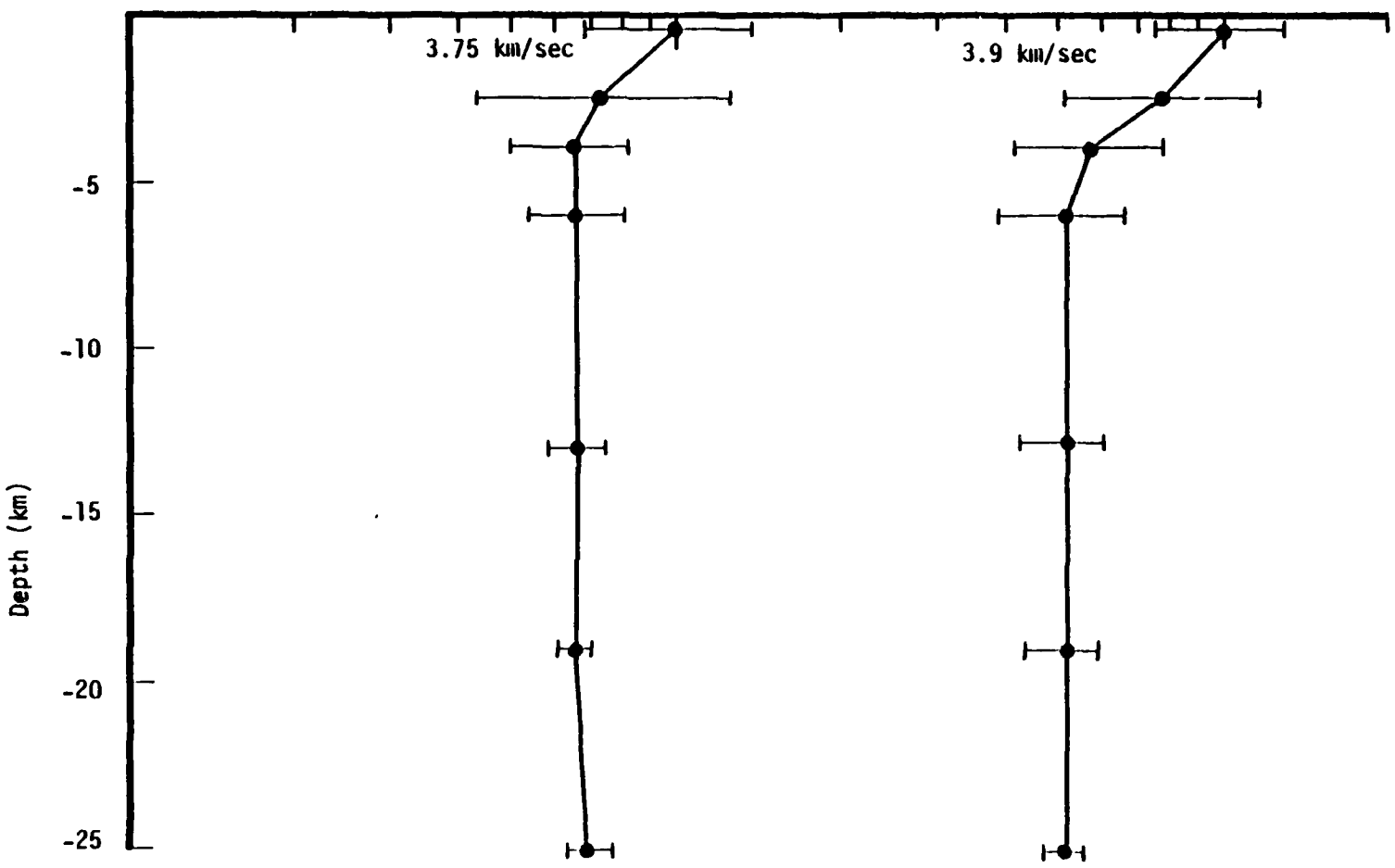

Figure 4. SV-radiation pattern averaged over a random distribution of focal mechanisms. Bars represent a standard deviation.

the other focal mechanisms considered (vertical strike-slip and the 45 degree thrust) are much more typical of what is to be expected for arbitrarily oriented focal mechanisms. On the average, we would expect Lg amplitudes to scale like m_b except for very shallow sources.

III. THEORETICAL Lg IN THE BASIN AND RANGE

3.1 INTRODUCTION

Many observational studies involving regional phases consider recordings from NTS explosions. It is important to understand regional propagation in this environment and how similar, or different, it may be from other types of crustal structures. In this section we will consider Lg propagation through Basin and Range type paths from NTS explosions.

There are reasons to expect that Lg may be a different type of wave propagation phenomena in the Basin and Range than in other crustal structures. It was found in Bache, et al. (1981) that group velocity corresponding to the Lg onset time for eastern United States crustal models and various Eurasian crustal models was closely related to the shear velocity at the basin crust. Analysis of the energies in the modes which make up Lg suggested that nearly all of the energy in Lg was distributed mainly in the lower part of the crust. The onset group velocities found for Lg tended to be within a few percent of the shear velocities in the crust, and the onset time was very similar to the onset time expected for a wide angle reflection of S-waves off the Moho. Lg onset group velocities for the Basin and Range are generally about 3.5 kilometers per second, very similar to values found for eastern United States. Yet, it is known from surface wave studies and seismic refraction work that the shear wave velocities of the Basin and Range crust are probably 3.9 or 4.0 kilometers per second. This is significantly higher than the Lg onset group velocity, and the patterns found in Bache, et al. (1981) relating Lg to properties of the lower crust are probably not appropriate in the Basin and Range. Here we will show that, unlike other crustal structures considered, Basin and Range Lg is basically a guided wave between the free-surface and an intermediate crustal reflector.

3.2 THEORETICAL MULTI-MODE RAYLEIGH WAVE DISPERSION IN THE BASIN AND RANGE

In this section we examine dispersion characteristics of multi-mode Rayleigh waves in Basin and Range type structures. The seismic velocities in the Basin and Range structure are well-known. The most detailed reference on this subject is the work of Priestley and Brune (1978) who use surface wave inversion results to obtain a detailed crustal structure for the Basin and Range. The Priestley and Brune structure, with some modifications at near the surface, is shown in Table 2. We have included at near the surface the Yucca Flat type structure of Bache, et al. (1978). Unlike any of the crustal structures studied in Bache, et al. (1980, 1981), the Basin and Range structure given here has a very distinct intermediate reflector at a depth of 25 kilometers.

Figure 5 shows the multi-mode Rayleigh wave phase and group velocities for this crustal structure. Note that the group velocity packet which we associate with Lg is in the range of 3.5 to 2.9 kilometers per second. This is a very similar range for that found for eastern United States. The major difference here, is that in eastern United States the upper range of the group velocity is very close to the shear velocity at the base of the crust. In this particular case, there are no group velocities which we would associate with Lg at all similar to the shear velocities at the base of the crust. Instead, in this case, the upper bound for the Lg group velocity appears to be related to the shear velocity just above the intermediate crustal reflector. For the Basin and Range, Lg appears to be somewhat different from that of eastern United States even though we will find a similar group velocity range which will be appropriate.

Figure 6 shows the distribution of kinetic energy with depth for a particular frequency for many modes. Note that a large packet of modes at this frequency has a concentration of energy in the layer just above the intermediate crustal reflector. This is very similar to the type of bunching of energy we have seen in Bache, et

TABLE 2

BASIN AND RANGE CRUSTAL STRUCTURES

Thickness	α	β	ρ	Q_ρ
0.30	0.58	0.90	1.65	20
0.075	2.29	1.21	1.73	20
0.225	2.13	0.99	1.70	20
0.325	2.50	1.43	1.90	50
0.25	4.40	2.75	2.40	75
1.125	5.00	3.10	2.40	100
2.00	5.50	3.20	2.60	200
20.70	6.10	3.51	2.82	400
10.00	6.60	3.85	2.84	600
29.00	7.80	4.50	3.30	1000

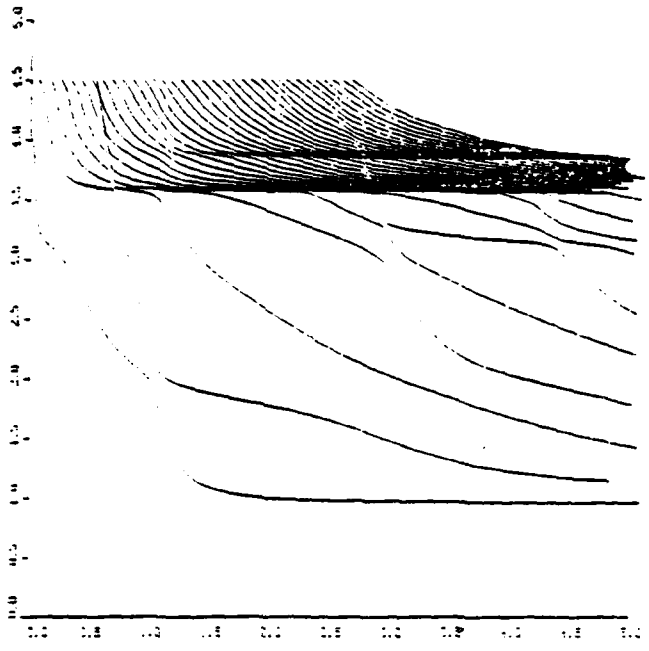

Phase Velocity

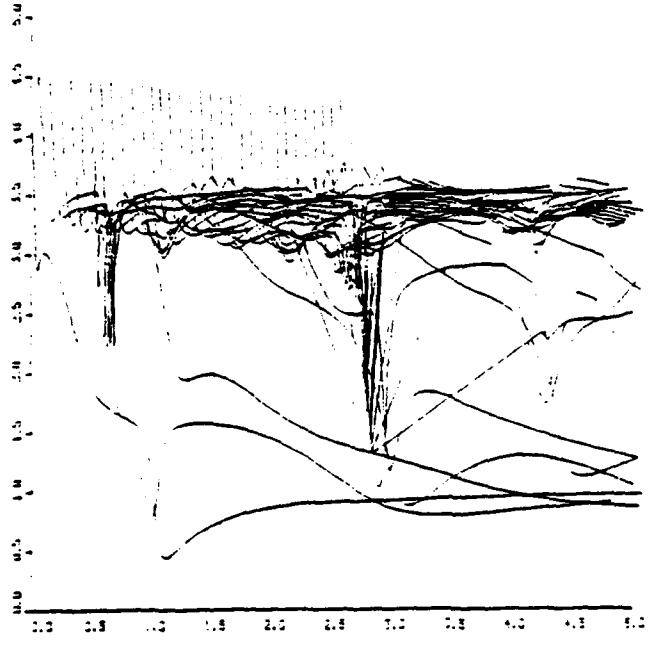

Group Velocity

Figure 5. Multi-mode Rayleigh wave phase and group velocities for Basin and Range crustal structure.

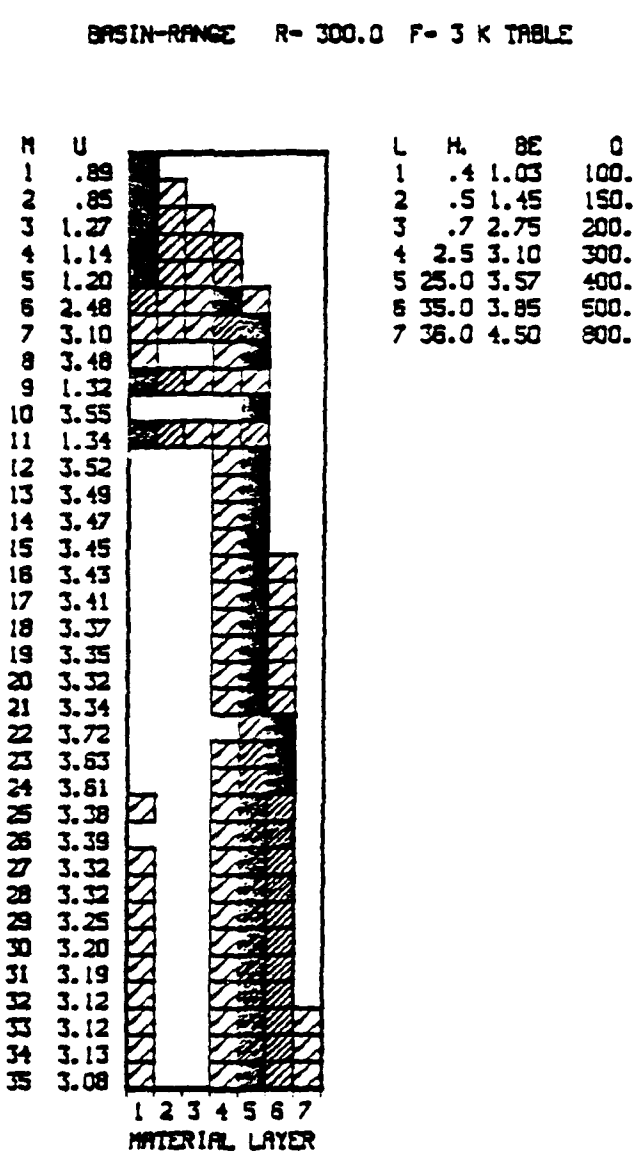

Figure 6. Distribution of model kinetic energy within the layers of the Basin and Range crustal structure for a frequency of 3 Hz.

al. (1981) for the eastern United States just above the Moho. This confirms our suggestion that Lg in Basin and Range is a slightly different phenomena than it is in the eastern United States. Most of the energy appears to be guided at shallower depths.

3.3 COMPARISON OF SYNTHETIC Lg WITH OBSERVATIONS FROM THE EXPLOSION DIABLO HAWK

In this section we compare synthetic Lg with Lg observed from the NTS explosion at DIABLO HAWK. A significant amount of anisotropic radiation was observed at DIABLO HAWK at low frequencies, and a significant amount of block motion was also observed in the vicinity of the source (Bache, et al., 1978). The event was covered by a large number of L^3 and S^3 short-period instruments (Figure 7). Here we will examine the recording made at Shellbourne, Nevada, at a range of 317 kilometers. Shellbourne was chosen because the path of propagation was entirely through the Basin and Range. Refraction work by Stauber and Boore (1980) suggests the crustal thickness is relatively constant over the path of propagation from NTS to Shellbourne.

Figure 8 shows the three-component S^3 recording at Shellbourne, Nevada. Note that the transverse component is larger than the vertical. The dominant motion is the radial motion. Lg is a very prominent phase. Its sharp onset corresponds to a group velocity of about 3.5 per second, and the coda contains a distinctive double burst of energy in the range of 3.5 to 2.9 kilometers per second in group velocity. This very distinctive feature is somewhat different from the characteristics of Lg seen in eastern United States.

Our interest here is in the propagation of characteristics of Lg in this particular crustal structure. Our modeling efforts are directed toward explaining the distinctive features of seismograms such as the onset time and the general coda shape. We will not be concerned with absolute amplitudes. The experience of Bache (1980, 1981) shows that the absolute amplitudes of short-period regional

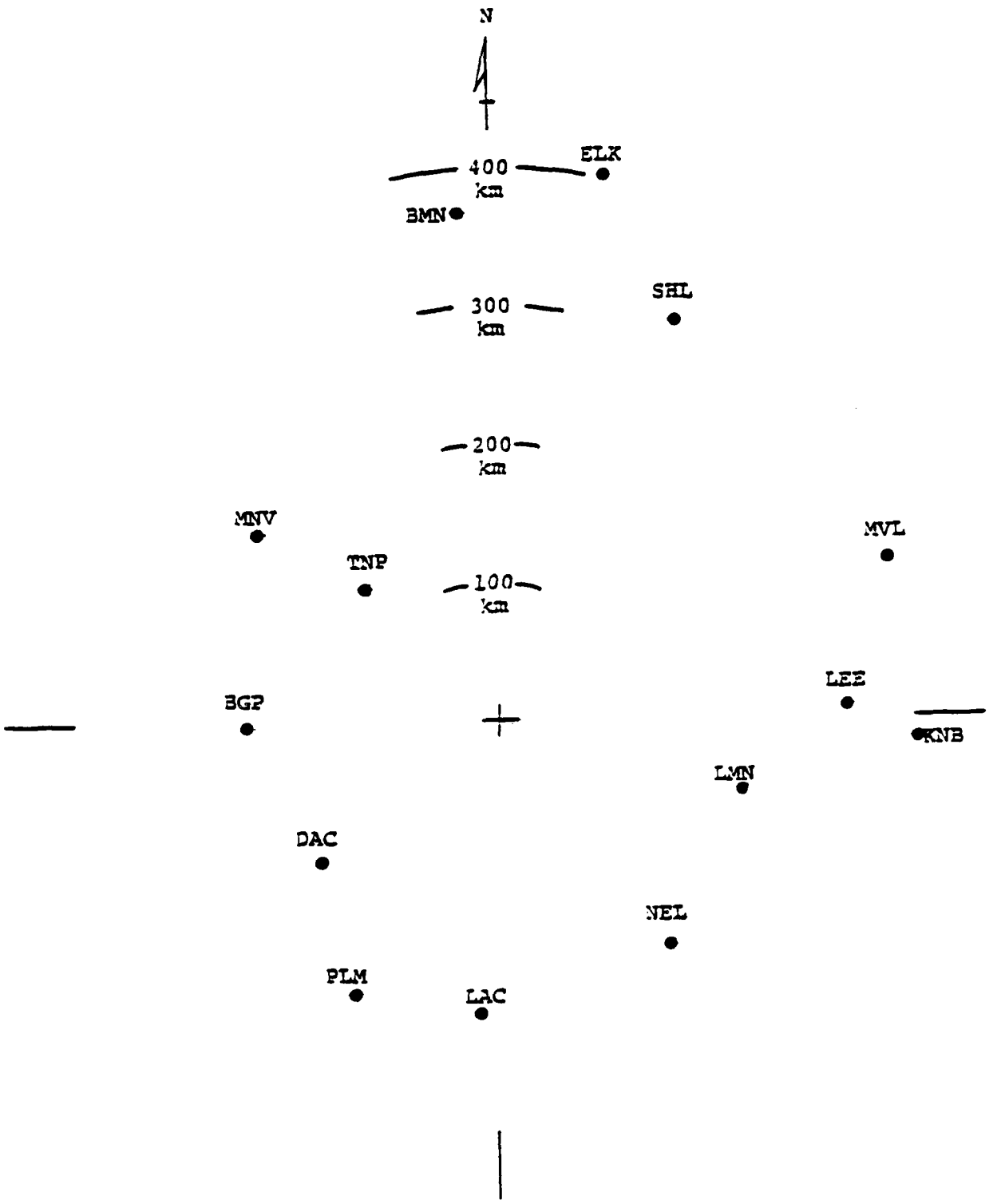

Figure 7. Regional stations recording the explosion DIABLO HAWK.

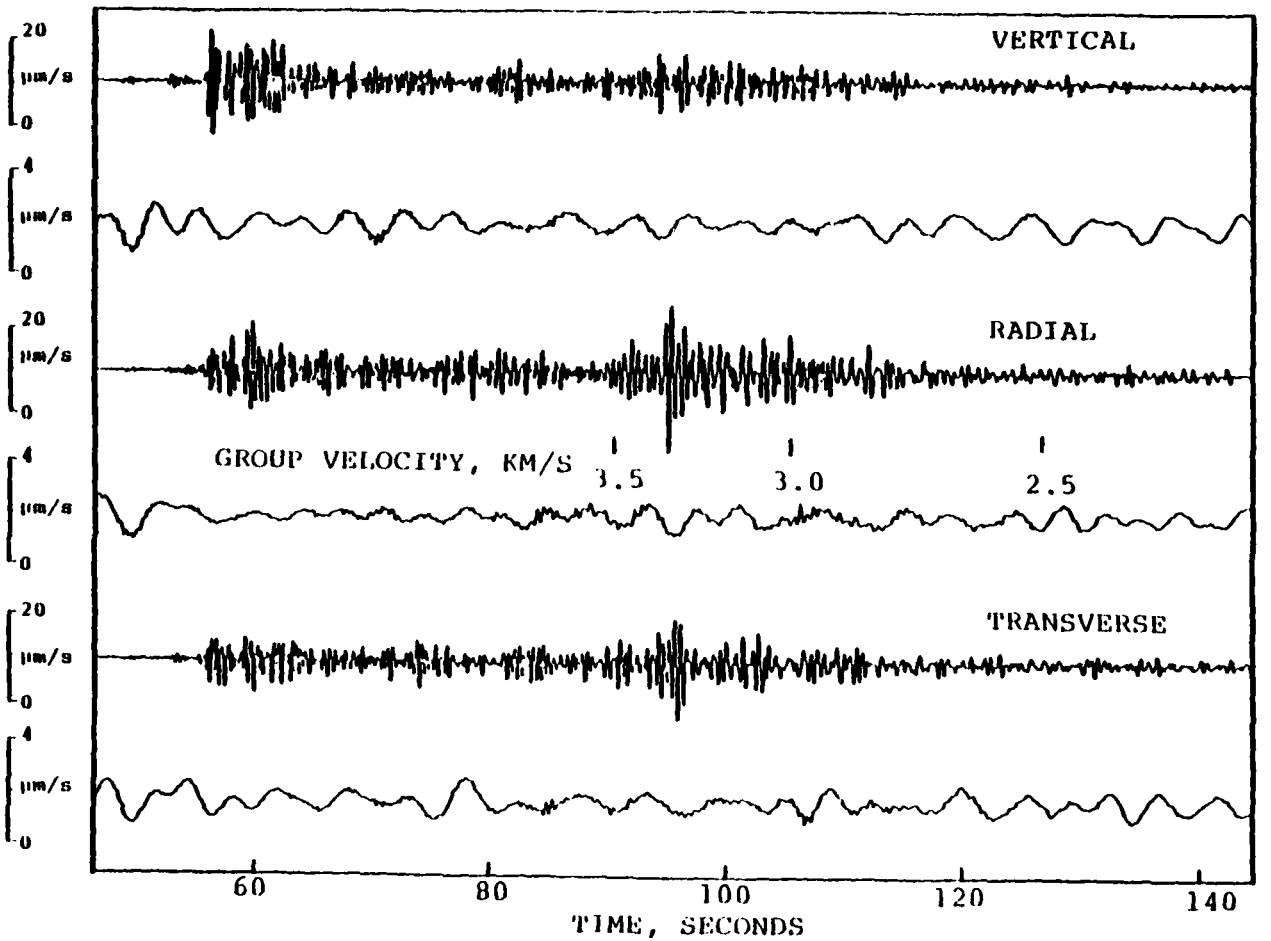

Figure 8. Three-component recording at Shellbourne, Nevada from DIABLO HAWK.

observations are very difficult to duplicate with synthetics in plane-layered earth models. Lg amplitudes appear to be sensitive to details of structure which cannot be obtained from simple refraction results and/or surface wave inversion studies.

As we have found from previous studies, published Q values for the bottom of the crust tend to be too low to allow Lg to propagate over large distances. The Q's near the surface tend to be too high, in that synthetic seismograms for shallow sources predict too much fundamental mode contribution. We have purposely reduced the shallow Q's significantly from published values to alleviate this problem. This is not to say that the intrinsic absorption of near-surface materials is necessarily significantly higher than what most models assume. We feel, from past studies, that the reason the fundamental mode is less prominent in data than in synthetics, is that scattering due to variations of near-surface materials is very important to the intermediate frequencies. Lg itself, which spends most of its time in the lower parts of the crust, is less sensitive to these features. Artificially low Q in the near-surface material is only used to suppress the fundamental mode. It does cause some suppression within the Lg, phase and group velocity range, but it is much less significant than resulting suppression of the fundamental mode. In terms of amplitude, the most important part of the crustal structure is the assumed Q as a function of depth. As summarized in Bache, et al. (1981), no plane-layered model employing linear intrinsic attenuation appears to be entirely satisfactory. There are probably physical effects occurring which cannot be simulated with such models, such as scattering.

Past results suggest that the best approach to modeling the observed time-domain characteristics of Lg is to employ a Q model with low Q (order 20) near the surface and high Q (order 1000) at the base of the crust and in the upper mantle. The low Q is needed to suppress the synthetic fundamental mode Rayleigh wave, which is not prominent in the time-domain data. The high Q in the deep crust is required by observed decay of amplitude with distance.

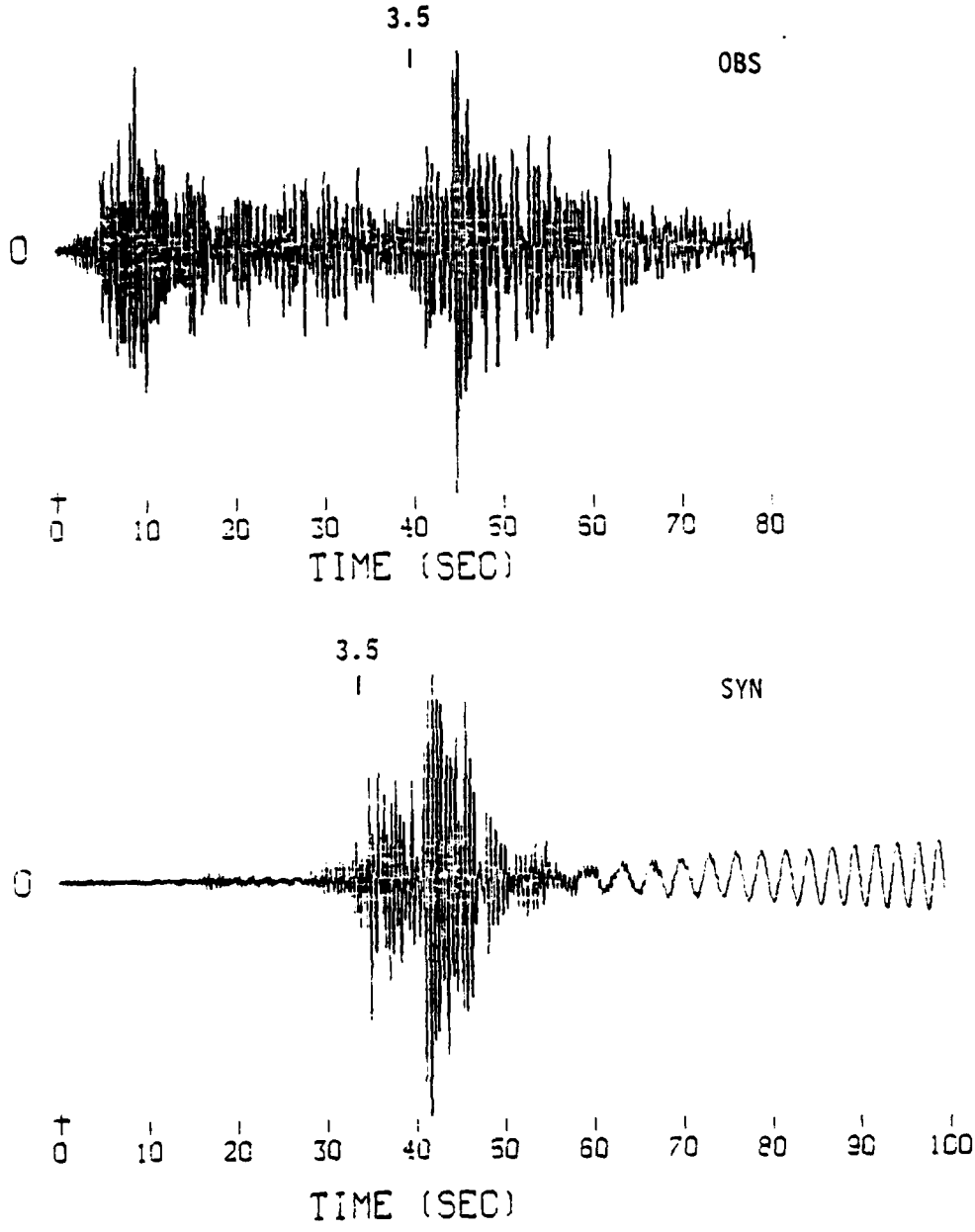

Figure 9. Comparison of synthetic at 300 km and observed radial component seismogram at Shellbourne at 317 km for DIABLO HAWK. The synthetic record is for an explosion (400 = 2200 m^3) plus a double-couple (moment = 1.8 x 10^{21} dyne-cm).

We have attempted to simulate the observed Lg at Shellbourne from DIABLO HAWK. The source used is a combined explosion and double-couple as determined by Bache, et al. (1979) A velocity structure for the Basin and Range crust was assumed, and the Q model was adjusted until the best fit was obtained.

Figure 9 compares the synthetic radial motion to the radial component observed at Shellbourne. Except for absolute amplitude, the comparison is quite good. Note that the Lg phase arrives at the correct time and the high-frequency codas of observed and synthetic records appear to have similar shapes. The double packet of energy observed at Shellbourne is included in the synthetic as well. The data contain somewhat more high frequency energy at late times than the synthetic, and the synthetic contains somewhat more low frequency energy at late times than the data. This presence of low frequencies is due to the fundamental mode which has not been totally suppressed. The absolute amplitudes are in error by about a factor of four. Considering experiences reported in Bache, et al. (1980, 1981), this discrepancy is not too surprising. The source excitation function used is simply a flat RVP spectrum. Including some overshoot in the source function might improve the agreement of the amplitudes.

We have demonstrated that the propagation characteristics of Lg in the Basin and Range are, to some degree, predictable and consistent with published crustal models. Difficulties in modeling Lg in the Basin and Range are similar to those found for other crustal structures.

3.4 SUMMARY

In this section we have briefly examined the propagation mechanism of Lg in the Basin and Range. Lg in the Basin and Range appears to be a somewhat different phenomenon from Lg in the eastern United States and Eurasian structures considered in our earlier studies. Theoretical calculations of dispersive characteristics of multi-mode Rayleigh waves suggest that the energy in Lg in Basin and

Range structure is actually trapped between the free-surface and an intermediate crustal refractor, and not between the free-surface and the Moho as in the other crustal structures. Therefore, we would expect the characteristics of Lg (and possibly other regional phases) in the Basin and Range to differ somewhat from Lg in other structures. This fact should be considered in discrimination studies; an observed relationship between regional phases in the Basin and Range may not be appropriate to other crustal structures.

We have used a slightly modified published crustal structure of Priestley and Brune (1978) to simulate the time-domain characteristics observed from the NTS explosion, DIABLO HAWK, at Shellbourne, Nevada, at 417 kilometers range. A distinctive shape seen in the data is mimicked to some degree by the synthetics, suggesting that the crustal structure of Priestley and Brune adequately describes the main propagation characteristics in regional phases. Crustal Q had to be modified in order to suppress the fundamental mode for a shallow explosion source. A poor choice for the Q model can make the fundamental mode quite large. The fundamental mode Rayleigh wave is still significantly larger in the synthetics in the data. Restricted to plane-layered models, as we are in these calculations, we have to suppress the fundamental mode through an artificially low Q, very high absorption, when actually the mechanism which may control the amplitude of the free-surface Rayleigh wave may be something very different than an absorption mechanism, such as a scattering mechanism. This is an inherent problem with any plane-layered calculation applied to large ranges.

IV. INVESTIGATION OF Lg SPECTRA AND CODA CHARACTERISTICS

4.1 INTRODUCTION

There have been a few instances where others have observed some differences between the spectral or coda characteristics of Lg generated by earthquakes and explosions which may suggest a discriminant. In this section, we use theoretical calculations of Lg to determine possible causes for these observed differences in earthquake and explosion generated Lg. There are two particular observations which we will examine in detail. The first is the observation by Rondout Associates (1980) that the distribution of energy within the Lg coda for earthquakes differs from the coda energy distribution for the nuclear explosion SALMON. Rondout observed more energy at later times in the Lg coda for SALMON than for moderate earthquakes in the eastern United States.

The second observation we wish to study is that of Murphy, et al. (1981) who examined the Lg spectra at the station TFO for various NTS explosions and earthquakes in the vicinity of NTS. Murphy, et al. observed that the ratio of high-frequency to low-frequency energy in Lg was greater for the earthquakes than for the explosions. This is somewhat surprising, considering that we normally expect the high-frequency generation of explosions to be more efficient than in earthquakes.

In both cases, the authors suggest the source-depth effect as a possible explanation for the observed phenomena. For Rondout's observation, it is suggested that the explosion source, being considerably more shallow than the average earthquake source, will generate more fundamental mode which tends to have slower group velocities than Lg, and this enhances the energy in the low group velocity window. For the case of the TFO observations made by Murphy, et al., it is suggested that the explosions, being more shallow, generate more fundamental mode which tends to enhance the low-frequency part of the spectrum. In this section we examine these hypotheses by computing synthetic seismograms for the two crustal structures of interest to investigate the cause of these

observations. We can use these results to determine whether these observations indicate an earthquake/explosion discriminant which may be used in other crustal structures, or whether the obervations are artifacts of the particular crustal structures or the particular source combinations which existed in the data sets examined in these two instances.

4.2 OBSERVED CODA DIFFERENCES IN EASTERN UNITED STATES

Rondout Associates (1980) observed a difference in the coda characteristics from the Lg from the nuclear explosion SALMON as compared to earthquakes in the same general crustal structure. The method employed by Rondout was very simple. The Lg observations were separated into two group velocity windows. A high group velocity window, with group velocities ranging from 3.9 to 3.4 kilometers per second, was compared to a low group velocity window from 3.4 to 2.9 kilometers per second. The energy in these two group velocity windows in the Lg coda was computed and ratioed. Figure 10 shows the ratio of the high-to-low group velocity window energy observed for SALMON compared to a few earthquakes from eastern United States. Note that in all cases there was a difference in the ratio of energy in the high-group velocity to low-group velocity windows for the two types of sources and with a fairly significant separation between the two populations. Generally, there is more late-arriving energy in the Lg coda for explosions than for earthquakes.

A possible explanation for this effect is that the explosions are, in general, shallower than earthquakes, and hence more efficient generators of the fundamental mode Rayleigh wave. The fundamental mode Rayleigh wave will generally have slower group velocities than Lg, and hence, force more energy into the late group velocity window. In our calculations, there is very little fundamental mode. The fundamental mode must be attenuated in order for synthetics to compare favorably to observed Lg singnals (Bache, et al., 1980). Even though there is little fundamental mode, there

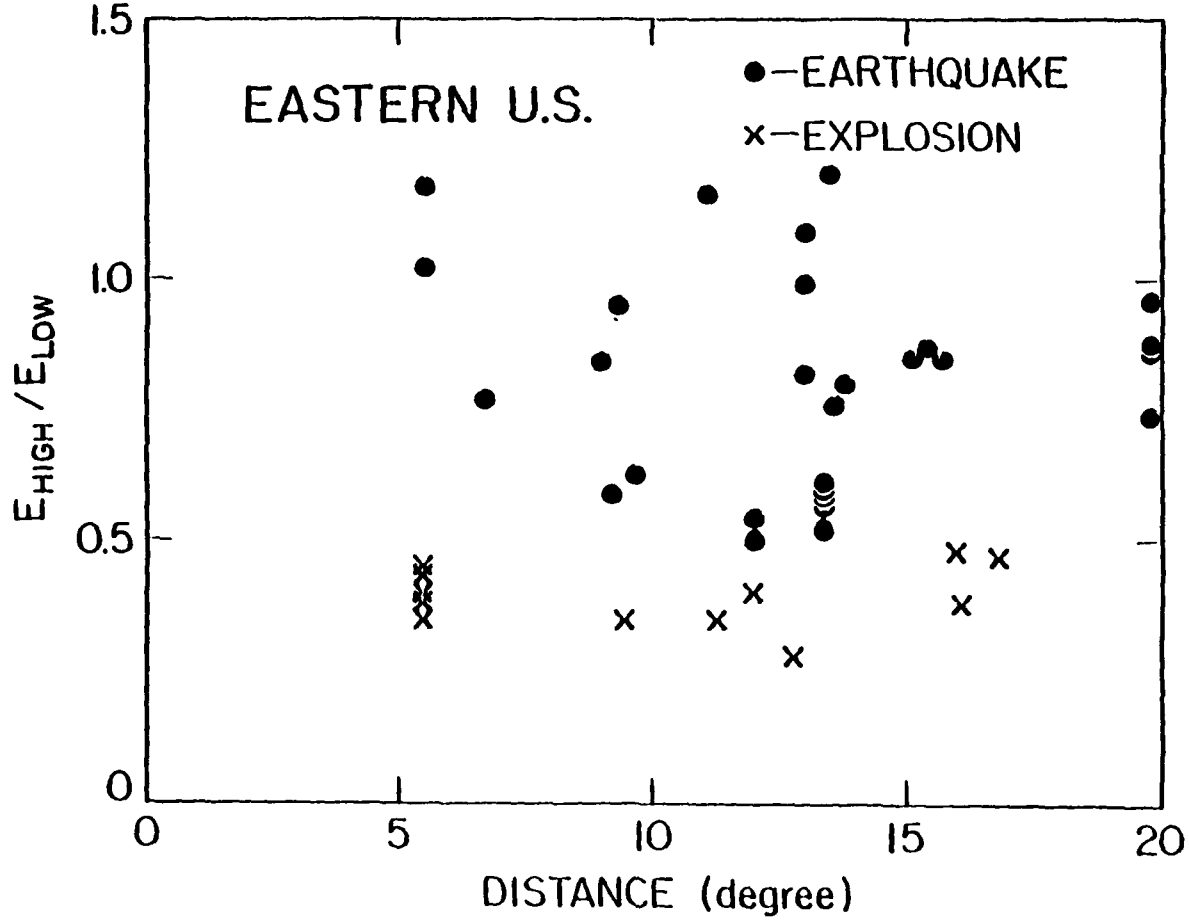

Figure 10. Ratio of Lg energy in high and low group velocity windows for explosions and earthquakes in eastern United States as determined by Rondout Associates (1980).

may be other modes which tend to travel slower than average and be excited relatively more by a shallower source.

On the other hand, this observation may be related to something other than the source-depth effect. There could be a distinctly different kind of excitation of the late arriving energy from the explosions than from earthquakes. It is this suggestion that we will examine. Suppose we consider a dislocation source and an explosion source at the same depth and compare the synthetic seismograms generated by both. Figure 11 shows the synthetic seismograms for the eastern United States structure (Table 1) for a source-depth of one kilometer for a vertical strike-slip source, a vertical dip-slip source and a point explosion. In each case, the same source spectrum is assumed; the spectrum is flat in reduced velocity potential, (RVP) for the explosion and flat in moment-rate for the two dislocation sources.

Note that the syntnetic for the explosion contains more late-arriving energy than the the synthetics for either dislocation source. Another mechanism, the 45 degree oblique thrust, generates a synthetic very similar to that of the vertical strike-slip and is not shown in the figure. Since the seismograms from any dislocation model can be made with a linear combination of the seismograms from the two orientations observed and a third orientation, which is essentially similar to the vertical strike-slip, it is fairly safe to assume that virtually all dislocation mechanisms will tend to have more energy theoretically toward the high group velocity end and relative to the low group velocity end compared to an explosion. Since these synthetics are made at the same source-depth, we obviously must come up with an explanation for this phenomena which is not related to source-depth. It must be some kind of phenomena associated with the differences in the excitation of Lg for an explosive source relative to a dislocation source.

For an idealized explosive source, all energy radiated in the source region is in the form of compressional waves, and any shear waves developed must come from interaction with boundaries or the

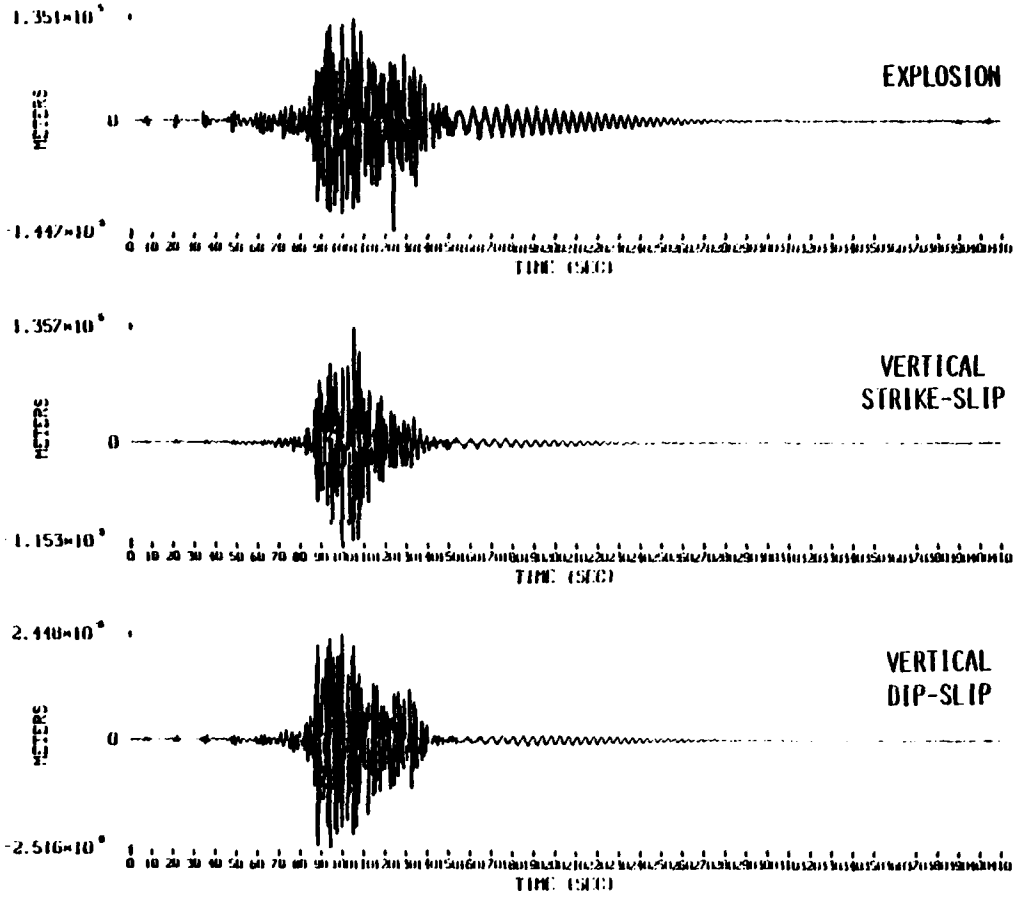

Figure 11. Synthetic Lg for explosion and double-couples with same source-time history and depth (800 m) in eastern United States structure.

free-surface. On the other hand, the dislocation source generates considerably more energy in shear waves than in the compressional waves, and we would expect the dominant contributor to Lg from dislocation sources to be the shear waves. However, propagating compressional waves in a layer must have phase velocities equal to, or exceeding, the P-wave velocity of the layer, whereas propagating shear waves can have velocities as low as the shear wave velocity of tne layer. For example, in the eastern United States crustal structure in Table 1, propagating compressional waves in layer two will have phase velocities exceeding 4.55 km/sec, whereas propagating shear waves can have phase velocities down to 2.54 km/sec. Therefore, a dislocation source located in layer two is likely to be more efficient than an explosion source in exciting modes with phase velocities lower than 4.55 km/sec. Thus, we would expect that an explosion would have a higher fraction of its total radiation in the high phase velocity range than would a dislocation at the same depth.

Thus, a possible explanation for the observation that explosions have more late-arriving Lg energy than earthquakes is that the high-phase velocity information, which is most prominent in explosions, is expressed in the lower group velocities in Lg. If one considers a tube wave analogy to the propagation of waves in the crust over large distances, the high phase velocities, meaning the steeper incident waves, will take many more multiple bounces on their way to the observer, and hence will have a slower group velocity. The question is whether such an analogy is appropriate to Lg.

In the high frequency limit, all modes beyond a certain order will have similar dispersive characteristics. The phase velocity and group velocity as a function of frequency will be the same except for a frequency shift. We can therefore arbitrar ly take out a high order mode and examine the behavior of phase velocity versus group velocity and assume that it is generally representative of all higner modes.

In Figure 12 we plot the phase velocity versus group velocity for the fifteenth higher mode in the eastern United States structure. For our hypothesis to be correct, we would expect that an increase in phase velocity would suggest a decrease in group velocity. Note that in the middle of the plot in the phase velocity range of 3.6 - 3.9 km/sec, we see exactly this trend. It may be that the observation made by Rondout that explosions generate more low group velocity energy relative to high group velocity energy than do earthquakes is simply a reflection of the fact that explosions generate relatively more high phase velocity energy than low phase velocity energy than do the earthquakes. This is only speculation and further study is needed to understand the observed phenomenon.

4.3 SPECTRAL DIFFERENCES OBSERVED FROM EARTHQUAKES AND EXPLOSIONS FROM THE NTS AREA

In this section we consider an observation made by Murphy, et al (1981) concerning the spectral characteristics of Lg observed at the station TFO from earthquakes and explosions in the NTS area. The Lg spectra from several earthquakes near magnitude four were averaged and compared with an average spectrum for explosions near magnitude four. The average earthquake and explosion spectra are plotted in Figure 13. Note that if one equalizes the frequency content at about 1 Hz, the earthquakes have considerably more energy in the 3 to 5 Hz range than the explosions. Here we compute synthetic seismograms and synthetic spectra for the Basin and Range structure described earlier for explosions and earthquakes which span the source-depths of interest.

Figure 14 shows the explosion spectrum for two different depths. Depths are 200 meters and 500 meters, and the source function has a flat spectral RVP at a range of 500 kilometers. Note that the spectral content is quite different for the two different source-depths. The low-frequency spectral amplitudes are slightly greater (relative to the high-frequency amplitudes) for the deeper source.

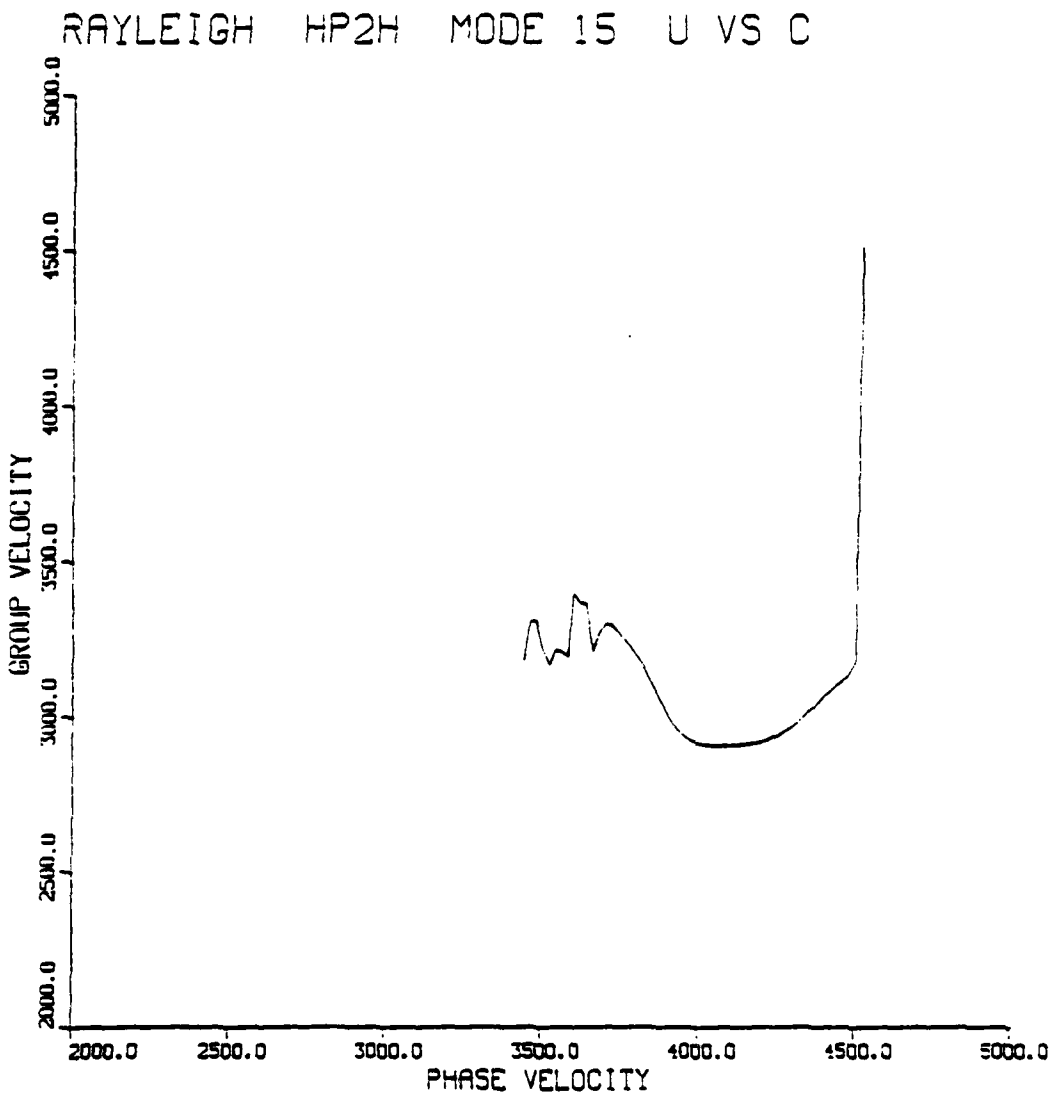

Figure 12. Phase velocity versus group velocity for the fifteenth higher Rayleigh mode in eastern United States structure.

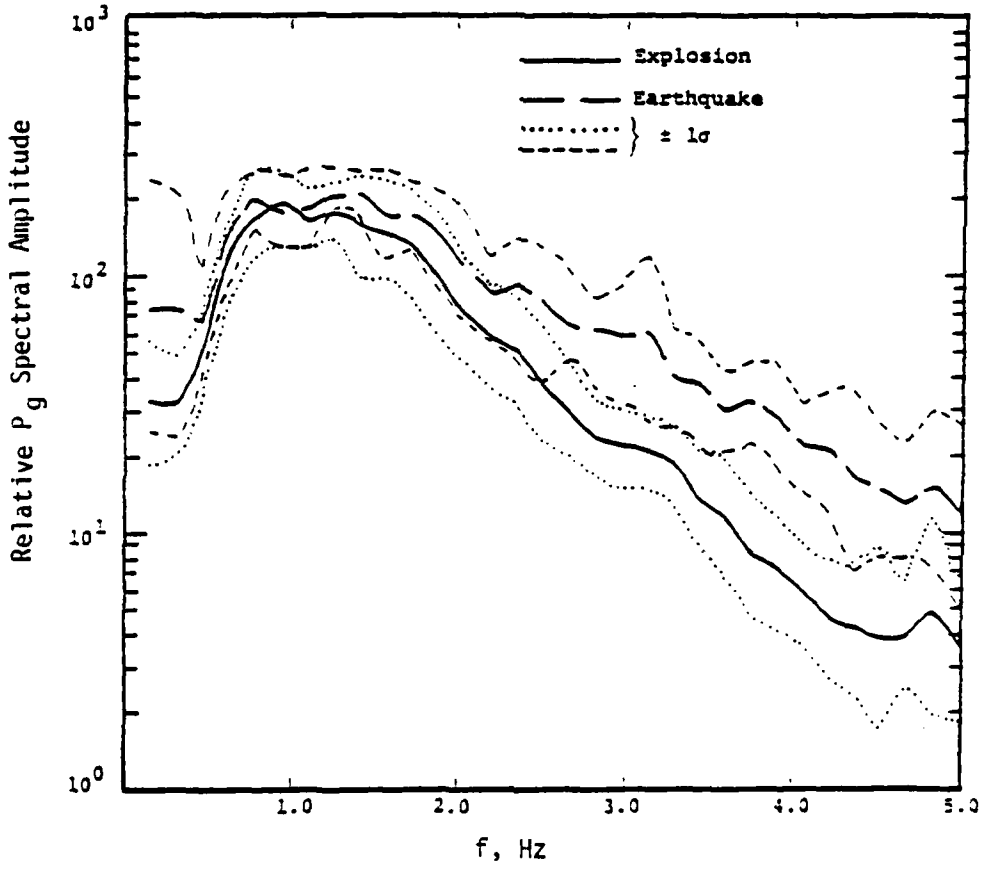

Figure 13. Comparison of normalized average spectra from earthquakes and explosions from the NTS area recorded at TFO (Murphy, et. al., 1981).

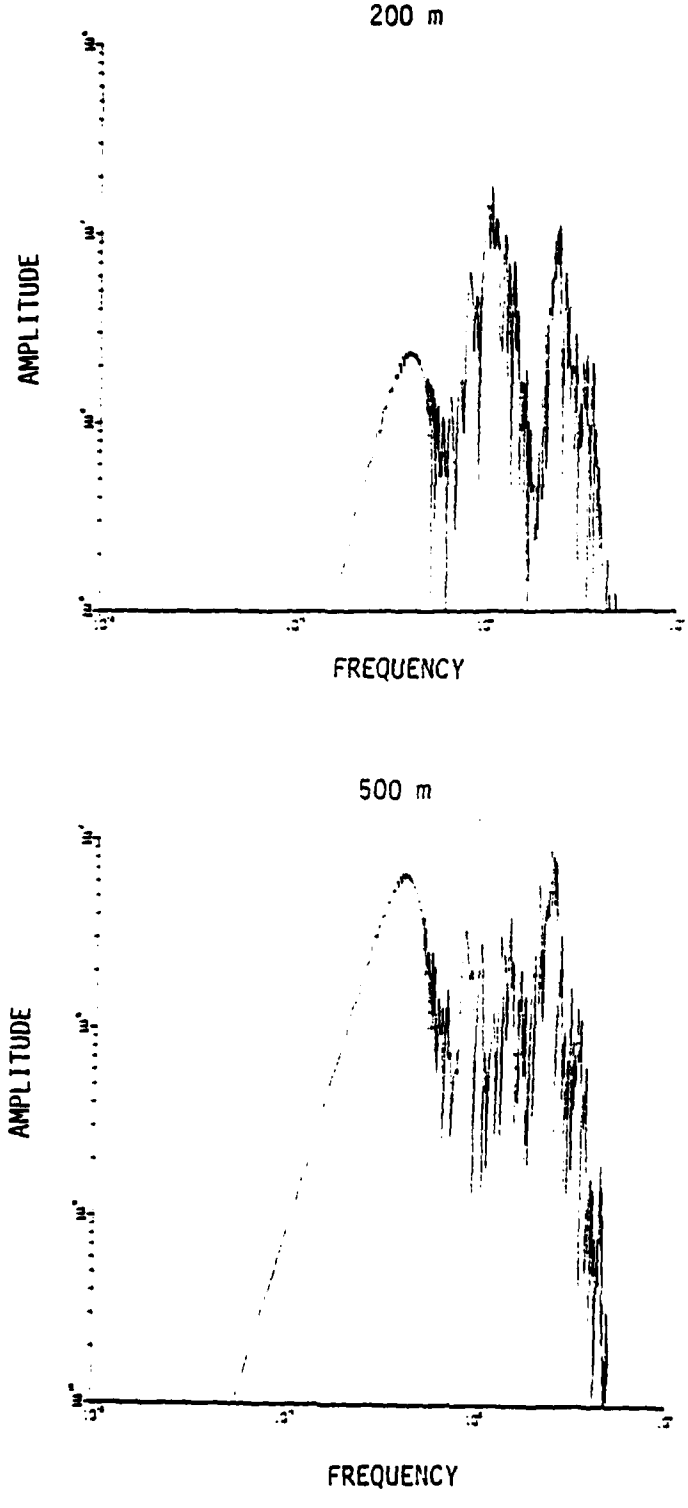

Figure 14. Synthetic Lg spectra for explosions buried at 200 and 500 m at a range of 500 km.

In Figure 15 we show the same type of spectral plot for double-couple sources located at source-depth of 4, 7, and 10 kilometers. In each case the source function is a step moment and the orientation is vertical strike-slip. Note that the spectral characteristics of the 4 kilometer deep strike-slip are very similar to the 200 meters deep explosion. In theory, there is no guarantee that shallower sources will necessarily generate more low-frequency energy than will deeper sources.

The difficulty in using synthetic seismograms from shallow sources is that amplitudes of the low frequencies of the synthetics are relatively arbitrary. They are determined primarily from the specification of the near-surface attenuation used in the calculations. As discussed earlier in Section III, we artificially reduce the Q in the near-surface materials to force the fundamental mode generated from shallow sources to be small. This is required by the short period data. Unfortunately we can make that amplitude arbitrarily small depending on just what levels of Q we choose. As also discussed in Section III, the artificial process of lowering the Q and hence increasing the absorption may be a poor representation of the actual physical mechanism. We are required, because of the use of plane-layered model, to use some mechanism like absorption and to eliminate the low frequencies so their time-domain signals small or incoherent. Other physical mechanisms may cause the low-frequency characteristics to be the way they are. For example, if the mechanism was truly a scattering mechanism where the fundamental mode is scattered by variations of near-surface structure along the path, we would expect the peak amplitudes to be reduced significantly, but, because of conservation of energy, the spectral amplitudes may be significant. This kind of phenomena is something we can not model with plane-layered seismograms.

The most appropriate explanation for the effects seen by Murphy, et al (1981) may indeed be a source-depth effect, but verification of this with our synthetic seismogram calculations is inconclusive at best. These particular calculations point out an

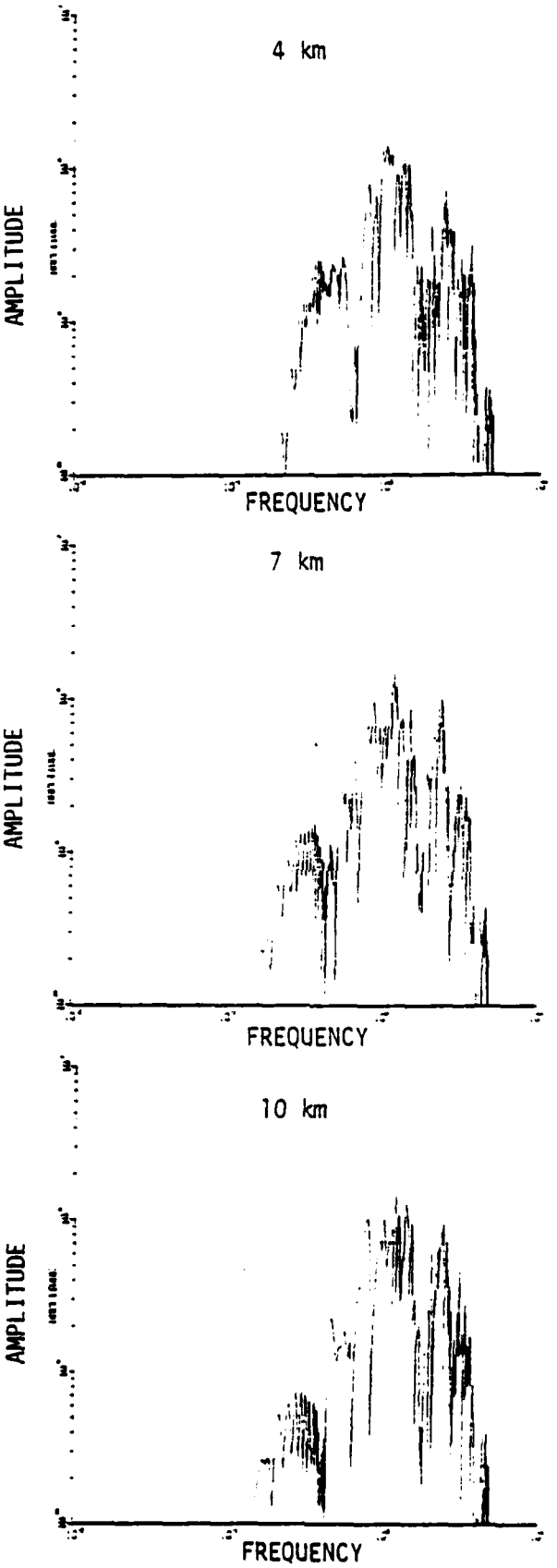

Figure 15. Synthetic Lg spectra for vertical strike-slip double-couples for three depths at a range at 500 km.

inherent weakness in the methods which we are employing. Namely we have no reasonable physical way of dealing with the coupling of the low frequencies observed through a short period instrument from shallow sources. We know from observations that this information cannot be coherent in the time-domain; so hence we artificially attenuate much of the energy in this frequency band. This energy may just be scattered to a point where it may be prominent in the frequency-domain while greatly dispersed and not obviously prominent visually in the time-domain. At present we can offer no suitable alternative for dealing with this particular problem and we should assume that this problem is inherent in all synthetic seismograms generating regional phases from very shallow sources.

4.4 SUMMARY

In this section we have examined two different observations relating the spectral and codal characteristics of Lg for explosions and earthquakes. The first case we examined is an observation by Rondout Associates which suggested that more late arriving energy was present in the Lg coda from the explosion SALMON than in the codas observed from the various earthquakes in the same crustal structure. It was speculated by Rondout that this effect may be a source-depth effect. The explosion, being more shallow than the earthquakes, in general, will generate more fundamental mode relative to the high frequencies which tends to travel at slower group velocities than Lg and hence will increase the slower moving amplitudes relative to the faster moving amplitudes. Here we computed synthetic Lg coda for double-couples of various orientations and explosions with the same effect of source-time history at the same depth. Our calculations show that the explosion does appear to generate more late arriving energy than the double-couple sources even for sources at the same depth. This suggests that it is not a source-depth effect Rondout is observing but some fundamental excitation difference between earthquakes and explosions.

The second case we examined is an observation made by Murphy, et al (1981) that the relative amounts of high-frequency to

low-frequency spectral content observed at TFO is different for earthquakes and explosions in the NTS area and, surprisingly, the earthquakes appear to have more high-frequency energy than do explosions. A possible explanation for this hypothesis is also source-depth effect, such that the explosions being shallower generate more fundamental mode and hence have relatively more low-frequency energy that the earthquakes. Calculations made to check this hypothesis have been inconclusive.

In plane-layer earth model calculations our only choice to keep the fundamental mode in the time-domain in reasonable amplitude relative to the high-frequency Lg is to include relatively low Q material low near the surface when considering shallow sources. It may be that mechanisms other than absorption are responsible for reducing the time-domain amplitudes of the fundamental mode. The most likely candidate is scattering due to variations in the near-surface material. We cannot model these in our calculations. Many of the characteristics of regional recordings, especially late arriving energy may be due to effects during propagation which cannot be modelled by plane-layered earth models.

V. PROPAGATION OF Lg ACROSS CRUSTAL STRUCTURE TRANSITIONS

5.1 INTRODUCTION

There are a few crustal structures in which Lg is not a prominent phase. Bache, et al (1981) examined two such structures to determine what may be the cause of the suppression of Lg. For the case of the oceanic structure they found that the gradients often present in the lower part of the crust are enough to cause large dispersion of Lg such that it is no longer a prominent phase. For the case of the Tibetan plateau, the few synthetic seismograms studied by Bache, et al. (1981) suggested that the crustal structure permits generation of an Lg-like phase. An alternative explanation must therefore be found for the absence of Lg as a prominent observed phase in the Tibetan plateau. One possible suggestion is that Lg is scattered at the boundaries of the Tibetan plateau which has a considerably thicker crust than the tectonic regions around it.

In this section we examine the possibility of scattering of Lg as it propagates from one crustal structure to another. We are primarily interested in whether sudden changes in crustal thickness can be sufficient to alter the character of the Lg such that it is no longer a prominent phase. Here we will use a method proposed by Alsop (1966) to approximate the propagation of Lg from one crustal structure to another. This method has been used by others to study the transition of the low-frequency fundamental mode and first higher mode across continent ocean margins. The method has not been used before to compute multi-mode synthetic seismograms.

We will consider propagation of SH-waves in very simple crustal structures. We will take a simple layer-over-half-space model and examine how the multi-mode SH-wave time histories vary as we propagate the signal into structures with increasing layer thickness. For economic reasons we will be considering fewer modes than we normally do for short-period regional applications. We will limit ourselves to the ten lowest modes and frequencies of approximately 0 to 1 Hz.

5.2 ALSOP'S METHOD

In this section we briefly summarize the method proposed by Alsop (1966) for the propagation of modal energy from one crustal structure into another. The method makes use of the orthogonality properties of modes and couples every mode in the initial crustal structure into every mode in transition structure. The initial modal system is propagated to the interface between the two crustal structures and is then decomposed into upgoing and downgoing waves. At the transition boundary these upgoing and downgoing waves are propagated across the boundary assuming plane wave reflection and transmission. The new system of upgoing and downgoing waves is then coupled back into the modes of the new crustal structure using the orthogonality conditions of Herrera (1964). Examples of applications of the method to Love and Rayleigh Wave problems can be found in Gregerson and Alsop (1974) and Chen and Alsop (1979).

Details of the theory and mathematics necessary for implementing the full three-dimensional problem is best described in Chen and Alsop (1979) and need not be repeated here. We will only discuss some of the considerations necessary for the specific problem we wish to address. Unlike previous applications, we are interested here in considerably higher frequencies and considerably more modes than have been considered in the past. For economic reasons we will consider only SH-wave propagation at normal incidence to the boundary between the two crustal structures. This makes the mathematics considerably easier and more manageable.

The most complicated part of the applicaton of the method is the computation of the effective reflection and transmission coefficients for one mode into the next. This is performed using the coupling formula of Herrera (1964):

$$\int_0 \sum_{q = x,y,z} [u_{qn}(z) \cdot \bar{p}_{xqm}(z) - \bar{u}_{qm}(z) \cdot p_{xqn}(z)]dz. \qquad (2)$$

Here the u_q are the three components of the displacement functions and the p_{xq} are the three components of the stress at the y - z vertical interface. m and n are the indices of two displacement-stress systems. The bars denote complex conjugate.

In previous applications of Alsop's method, this coupling equation, which involves an integral over all depth, was evaluated numerically. For high-frequency modal problems this is quite difficult. One reason is that the integrals must be sampled quite finely, and, also, in modal calculations the computation of the high-frequency eigen-functions is often unstable when using classical calculation methods. Here we have improved upon past efforts by stabilizing the calculation by evaluating this integral analytically. The upgoing and downgoing wave field and as well as the eigen-functions within each layer can be expressed by the sum of the upgoing and downgoing waves which can be either propagating or evanescent. In each layer we have analytically solved the cross product inside the Herrera integral and evaluated the integral analytically in a form which can be numerically evaluated in a stable manner.

Even though we have simplified the problem by adding the analytic solutions, the computations are still quite tedious. Every mode in one crustal structure must be coupled into every other mode in the second crustal structure. Therefore the number of computations made is related to the number of modes squared. Normally when constructing Lg seismograms, we use as many as 35 to 50 modes to span a frequency out to about 5 Hz. In this case, using that many modes would be prohibitively expensive. Therefore we restrict it to a few number of modes, in this case, about ten. Even using only ten modes, the cost for computing one seismogram through simple transition structure is considerably more than that for the fifty mode Rayleigh seismograms that we computed for many layer crustal structures.

5.3 APPLICATION OF THE METHOD TO TRANSITION ACROSS VARYING CRUSTAL THICKNESS

To examine the effect of changing crustal thickness on Lg propagation we choose a very simple case to examine. We assume the crustal layer has a shear velocity of 3.55 km/sec and a density of 2.7 gmk/cm^3. The half-space has velocity and density of 4.5 km/sec and 3.3 gm/sec^3. We consider only single layer over half-space crustal structures. We will place the source in one structure and compute the propagation in the crustal structures of different crustal thickness. This problem is very simple and the only parameter which is changed from case to case is the crustal thickness. We will get a good indication of the effect of that single parameter.

It has been shown by Herrmann (1977) and Swanger and Boore (1978) that the SH modal contribution for crustal structures like this and at the ranges that we will consider is a very good approximation to the complete response. Interestingly for the problems which we will consider, there is one part of the solution which should remain unchanged going from one crustal structure to the next, and that is the direct wave from source to receiver. In our calculations we could use the direct wave as a reference point. It will be a reference for how well the actual Alsop coupling method works, since if it worked exactly it should preserve the amplitude of the direct wave. Also the direct wave acts then as a reference to the other parts of the wave frame in terms of how much the signal may have been altered.

In Figure 16 we give a graphic display of the transmission coefficients of modes of the initial structure coupled into each mode of the second structure for the case of modes propagating from a 30 kilometer crust to a 40 kilometer crust. Note that a single mode in the initial structure does not couple to only one mode in the second structure. It spreads its energy over many modes. In general though there is a range of maybe four or five modes for which transmission of a single mode is most efficient. One could

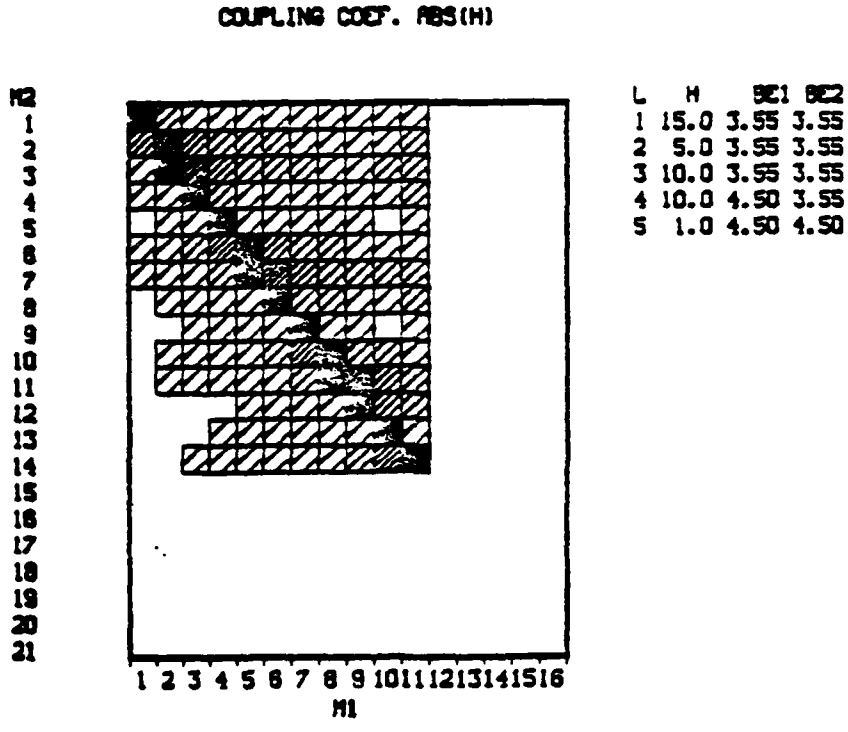

Figure 16. Transmission coefficients for Lg propagation from a 30 km crust onto a 40 km thick crust.

simplify the calculations by disregarding modes very far away from where we would expect the coupling to be the maximum. In the cases to follow we have not done that, and in general, we found no particular way of estimating exactly which modes should be considered without computing all ot the coupling coefficients.

First we consider propagation from a thin crust into thicker crusts. Our source will be a 5 kilometer buried double-couple structure with thickness of 30 kilometers. We compute synthetic seismograms at a range of 200 kilometers observed in structures with crustal thickness of 40 to 60 kilometers. Half of the propagation of the initial structure and half are in the structures with thickening crusts.

Figure 17 shows seismograms for the three cases considered. Note that the peak amplitudes are virtually the same for all three cases. As mentioned above if the coupling were exact we would expect the direct wave from source to receiver to be identical in all three cases. The Alsop method appears to perform very well here since the amplitude varies by only a few per cent for the largest motion which is due to direct wave. Note that the early part of the coda which includes approximately five or six multiple bounces in the crustal structure has hardly changed at all by the transition. The late part of the coda diminishes an amplitude by a great deal, almost in order of magnitude from the 40 kilometer case to the 60 kilometer case. We can conclude that some of the coda will be changed drastically and probably reduced by the transition from one crustal thickness to another if the thickness difference is extreme.

We would also expect the early arrivals to be altered as well if there is any kind of impedence contrast within the crust at crustal depths between the two crustal units. But considering that so much of the early part of the coda is preserved in these comparisons, it is doubtful that the transition will be totally destructive on the signal. The direct wave which we have present here is something we probably would not see in real data. But

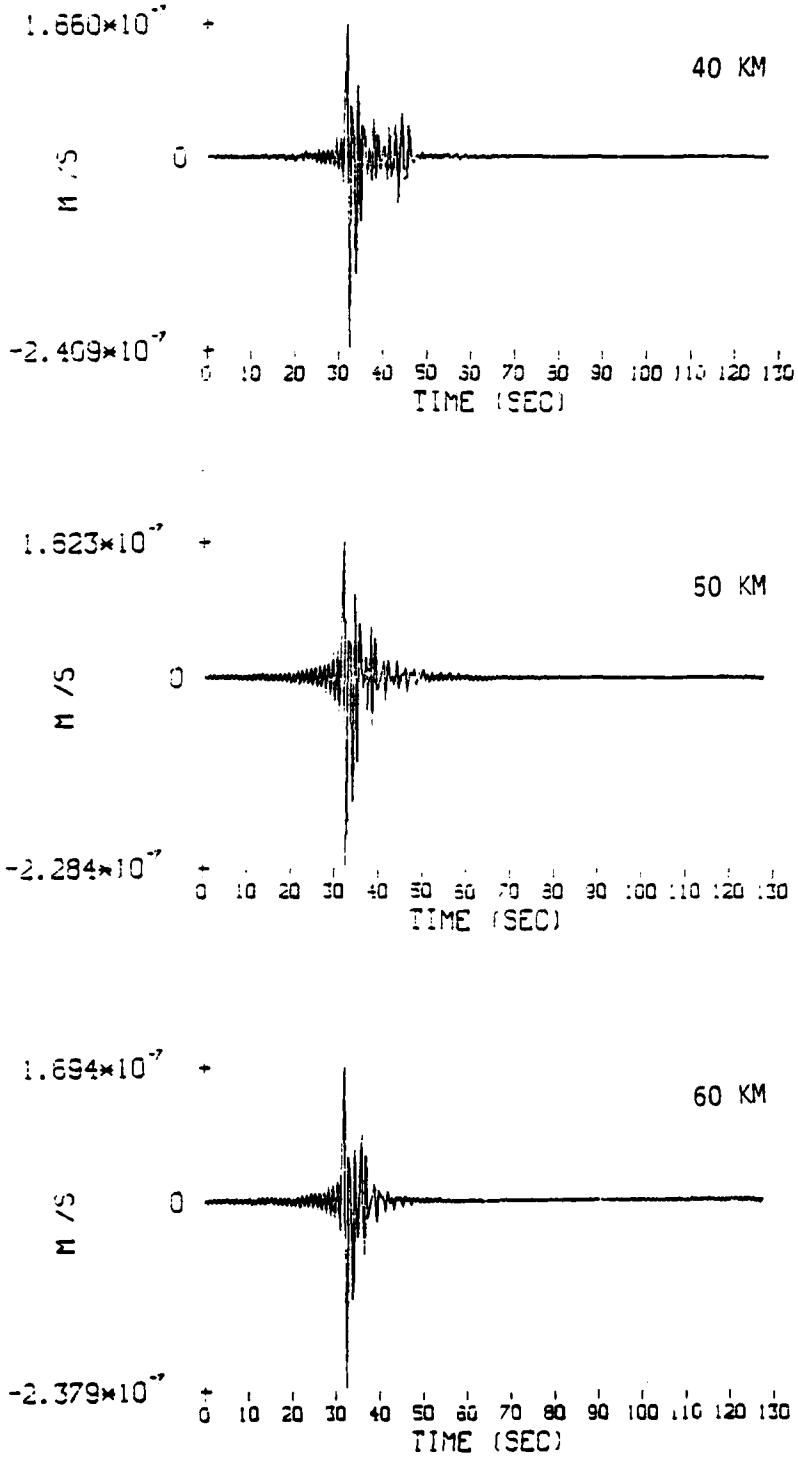

Figure 17. SH-wave seismograms generated in a 30 km thick crust and observed after transition to thicker crusts.

considering the size of the arrivals coming just after the direct wave suggest that much of the energy will propagate fairly efficiently into the new crust.

Next we consider propagation in the opposite direction with the sources located in the thicker crusts and propagate to the thin crusts. The ranges considered will be the same and the crustal depth and source type will also be the same. Figure 18 shows the seismograms with the three cases where the source is in the 40, 50, and 60 kilometer crust and the observer in each case is in a 30 kilometer crust. The effects on the signal are similar to the previous case. The early arrivals are altered but very slightly; but the late arriving energy is reduced considerably. Again, the Alsop method preserves the direct wave quite well.

5.4 SUMMARY

We have used the method of Alsop (1966) to propagate SH-wave codas from one crustal structure to another to assess the effect of varying crustal thickness on Lg codas. We have considered only the simplest case: the single layer over a half-space structure, and layer thickness is the only parameter varied in the problem. The effect of changing crustal thickness is very similar for both directions of propagation. Substantial changes in part of the wave form take place only when the crustal thickness change is quite large, of the order of a factor of two. Change in crustal thickness of one part in three appears to make very little difference. The general coda characteristics for propagation from a 30 to 40 or 40 to 30 kilometer crust were neglible in terms of the amplitudes over the entire coda.

We can conclude that changing crustal thickness certainly does have an effect on the actual wave forms when the thickness change is large; but it is not a completely destructive effect. Even if we remove the direct wave, which should be preserved in all the calculations, there is still a significant part of the coda which survives slightly altered and with considerable amplitude after

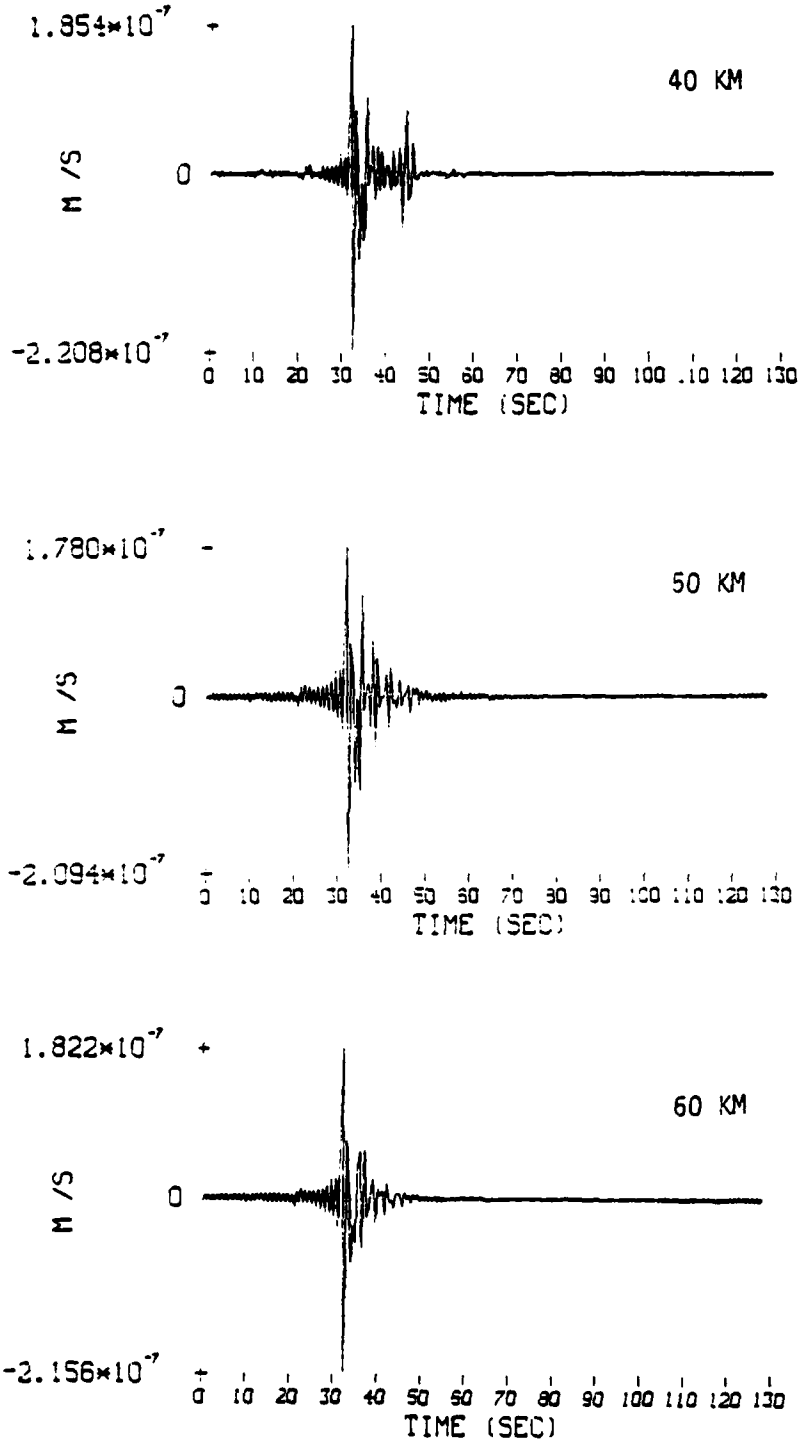

Figure 18. SH-wave seismograms generated in thicker crusts and observed in 30 km thick crust.

propagation across the crustal transition zone. The later the arriving energy, the more the wave forms are altered and the amplitude is diminished.

There is a possibility that we are considering too low frequencies to model what might affect Lg propagation at the frequencies normally seen on a short period seismograph, namely 1 to 5 Hz. It may be that the higher frequencies will be dispersed more and will be reduced in amplitude more than the lower frequencies shown here. One may also argue that these results may not be valid to the Lg problem because we are considering only very simple crustal structures. But if we examine the crustal structures normally given for Eurasia, they are equally as simple. Generally, published Eurasian crustal structures have only two or three layers over a half-space. We would expect that using those crustal structures for a study like this the results would be very similar.

VI. SUMMARY OF TRES CODE DEVELOPMENT ON THE CRAY-I COMPUTER

TRES is a three-dimensional, small-strain, explicit finite difference code which has been made operational on three computers, the ILLIAC IV, a UNIVAC 1100/81, and, more recently, a Cray-1. The Cray-1 version was developed during FY '80 using a Cray computer at the National Center for Atmospheric Research (NCAR). A partial vectorization of the code was undertaken, and the resulting code performance was described by Bache, et al. (1981). In general, it was found that TRES performed three-dimensional simulations approximately as fast on the Cray as it had on the ILLIAC. Furthermore, it was estimated that a complete optimization for the Cray would yield approximately a four-fold increase in computing speed.

The current contract provided for a ten man week effort to upgrade the modeling capability of TRES on the Cray computer. We have: (1) modified the code to accommodate nonhomogeneous material properties, (2) incorporated a spontaneous-rupture earthquake model, and (3) developed an algorithm to simulate earthquake faulting which outcrops at the free surface. These modifications have been programmed at NCAR, and a series of test problems have been successfully performed to validate the modified code.

The new fault plane algorithms are described in Appendix A which was prepared by Boris Snkoller and Steven Day. The algorithms were tested by comparing numerical results with previous numerical solutions obtained on the ILLIAC. The results agreed to more than four decimal places, as expected, since the new algorithms are algebraically equivalent to those programmed for the ILLIAC during FY '80 (see Bache, et al., 1980).

VII. SUMMARY

This report summarizes efforts to simulate the characteristics of regional seismic phases from earthquakes and explosions and to modify existing three-dimensional finite difference codes for use on the Cray-1 computer.

In Section II the depth dependence of the phase Lg is examined. Previous studies had found that the depth dependence of Lg for dislocation sources was highly source mechanism dependent. It was found here that the depth dependence of Lg seen in synthetic seismograms for double-couple sources can be explained by changes in material properties over crust depths, and radiation pattern effects of S-waves radiated with the phase velocities appropriate to Lg. One of the mechanisms considered by Bache, et al. (1981) is very anomalous, and probably not representative, of a typical earthquake source. On the average it was found that the amplitudes of Lg as a function of depth should scale much like m_b except for very shallow sources.

In Section III Lg propagation in the Basin and Range tectonic province was examined. It was shown that the mechanism of Lg propagation in this environment is different from that of other crustal environments examined by Bache, et al. (1980, 1981). For eastern United States and Eurasian crustal structures, Lg was found to be a guided wave between the earth's surface and the Moho. For the Basin and Range, most of the energy is trapped above an intermediate crustal reflector. This suggests that the characteristics of Lg propagation in the Basin and Range may be different from that in other crustal structures, and observations made that environment may not be appropriate to other tectonic provinces.

In Section IV we examine two observations made concerning differences in the characteristics of Lg radiated from earthquakes and explosions. Rondout Associates (1980) observed more late ariving energy relative to early arriving energy from the explosion SALMON than for earthquakes in eastern United States. Synthetic

seismograms for eastern United States crustal structure also show this feature, but it is found not to be a source-depth effect, as previously suggested. Explosion sources give more late arriving energy than double-couple sources at the same depth and with the same effective source-time histories. We also investigated an observation by Murphy, et al. (1981) who observed spectral differences in Lg spectra for explosions and earthquakes from the area of NTS. They found earthquake spectra to have relatively more high frequency content than explosion spectra. Synthetic Lg spectra cannot conclusively support the observations in this case. The low frequency energy in synthetic Lg for shallow sources is largely artificial. Plane-layered earth models appear to be insufficient for describing the behavior of Lg in this case.

In Section V we employed the method of Alsop (1966) to investigate the behavior of Lg codas as they are transmitted across boundaries between two different crustal structures. Of particular interest was crustal structures with very thick crusts in which Lg is often not an important phase. It is found that large changes in crustal thickness, which has been suggested as a reason why Lg is not prominent in some tectonic provinces, is not sufficient to explain a disappearance of Lg. Some destructive effect is found, but not enough to eliminate the phase completely. We suspect that other circumstances lead to the destruction of Lg, such as high crustal intrinsic attenuation or scattering.

VIII. REFERENCES

Aki, K. and P. G. Richards (1980), Quantitative Seismology: Theory and Methods, W. H. Freeman and Co., San Francisco.

Alsop, L. E. (1966), "Transmission and Reflection of Love Waves at a Vertical Discontinuity," JGR, 71, 3969-3984.

Bache, T. C., J. T. Cherry, D. G. Lambert, J. F. Masso and J. M. Savino (1976), "A Deterministic Methodology for Discriminating Between Earthquakes and Underground Nuclear Explosions," Systems, Science and Software Final Technical Report, SSS-R-76-2925.

Bache, T. C., W. E. Farrell and D. G. Lambert (1979), "Block Motion Estimates from Seismological Observations of MIGHTY EPIC and DIABLO HAWK," Systems, Science and Software Final Technical Report, DNA 001-77-C-0260.

Bache, T. C., H. J. Swanger and B. Shkoller (1980), "Synthesis of Lg in Eastern United States Crustal Models," Systems, Science and Software Semiannual Technical Report, SSS-R-81-4668, September.

Bache, T. C., H. J. Swanger, B. Shkoller and S. M. Day (1981), "Simulation of Short Period Lg, Expansion of Three-Dimensional Source Simulation Capabilities and Simulation of Near-Field Ground Motion from the 1971 San Fernando, California Earthquake," Systems, Science and Software Final Report sponsored by ARPA, SSS-R-81-5081, July.

Chen, T. C. and L. E. Alsop (1979) "Reflection and Transmission of Obliquely Incident Rayleigh Waves at a Vertical Discontinuity Between Two Welded Quarter-Spaces," BSSA, 69, 00. 1409-1424.

Cherry, J. T. (1977), "User's Manual for the TRES Code," S-Cubed Report, SSS-R-77-3128.

Coleman, P. L. , S. M. Day, N. Rimer, J. T. Cherry, J. R. Murphy, and T. C. Bache (1979), "Small-Scale Explosion Experiments, Seismic Source Calculations and Summary of Current Research," S-Cubed Report, SSS-R-79-4023.

Gregersen, S. and L. E. Alsop (1974), "Amplitudes of Horizontally Refracted Love Waves," BSSA, 64, 535-553.

Herrera, I. (1964), "On a Method to Obtain Green's Function for a Multilayered Half-Space," BSSA, 54, 1087-1096.

Herrmann, R. B. (1977), "Research Study of Earthquake Generated SH Waves in the Near-Field and Near-Regional Field," Final Report, Contract DACW39-76-C-0058, Waterways Experiment Station, Vicksburg, Mississippi.

Murphy, J. R., T. J. Bennett, and T. K. Tzeng (1981), "Spectral Characteristics of Short-Period Regional Phases Recorded from NTS Explosions and Earthquakes," (Preprint) Presented at the Annual Meeting of the Eastern Section of the Seismological Society of America, October.

Preistley, K. and J. Brune (1978), "Surface Waves and the Structure of the Great Basin of Nevada and Western Utah," JGR, 83, 2265-2272.

Rondout Associates, Inc. (1980), "Regional Seismic Wave Propagation," Final Technical Report sponsored by ARPA, F49620-78-C-0043.

Swanger, H. J. and D. M. Boore (1978), "Simulation of Strong-Motion Displacements Using Surface-Wave Modal Superposition," BSSA, 68, 907-922.

APPENDIX A

FAULT PLANE TREATMENT FOR MULTIMATERIAL TRES

APPENDIX A
FAULT PLANE TREATMENT FOR MULTIMATERIAL TRES

This appendix outlines modifications to the Cray version of the TRES code necessary for properly treating shear failure in three dimensions. The treatment is general enough to accommodate material heterogeneity and zone-size nonuniformity in the vicinity of the fault plane. Interaction of the fault plane with grid boundaries, including the free surface, is also permitted.

The physical basis of the fault plane treatment is given by Coleman, et al. (1979). All notation not defined in this appendix is that of the TRES User's Manual (Cherry, 1977), except that all stresses σ have had the prestress subtracted off. Let Γ_{xz} and Γ_{yz} be the prestresses at a given node on the fault plane. Then define $SACC^+$, $XACC^-$, $YACC^+$, and $YACC^-$ at that node:

$$XACC^+ = \frac{(\sigma_{xx})_{AB}\,(1-\xi^y)}{(\rho_A\Delta x^+ + \rho_B\Delta x^-)} + \frac{(\sigma_{xx})_{DC}\,\xi^y}{(\rho_D\Delta x^+ + \rho_C\Delta x^-)}$$

$$+ \frac{(\sigma_{xy})_{AD}\,(1-\xi^x)}{(\rho_A\Delta y^+ + \rho_D\Delta y^-)} + \frac{(\sigma_{xy})_{BC}\,\xi^x}{(\rho_B\Delta y^+ + \rho_C\Delta y^-)}$$

$$+ \frac{\left[(\sigma_{zx})_A + \Gamma_{zx}\right]}{\rho_A\,\Delta z^+}(1-\xi^x)(1-\xi^y) + \frac{\left[(\sigma_{zx})_B + \Gamma_{zx}\right]}{\rho_B\,\Delta z^+}\xi^x(1-\xi^y)$$

$$+ \frac{\left[(\sigma_{zr})_C + \Gamma_{zx}\right]}{\rho_C\,\Delta z^+}\xi^x\xi^y + \frac{\left[(\sigma_{zx})_D + \Gamma_{zx}\right]}{\rho_D\,\Delta z^+}(1-\xi^x)\xi^y + fx^-$$

$$XACC^{-} = \frac{(\sigma_{xx})_{EF}}{(\rho_E \Delta x^{+} + \rho_F \Delta x^{-})} (1 - \xi^y) + \frac{(\sigma_{xx})_{HG}}{(\rho_H \Delta x^{+} + \rho_G \Delta x^{-})} \xi^y$$

$$+ \frac{(\sigma_{xy})_{EH}}{(\rho_E \Delta y^{+} + \rho_H \Delta y^{-})} (1 - \xi^x) + \frac{(\sigma_{xy})_{FG}}{(\rho_F \Delta y^{+} + \rho_G \Delta y^{-})} \xi^x$$

$$- \frac{(\sigma_{zx})_E + \Gamma_{zx}}{\rho_E \Delta z^{-}} (1 - \xi^x)(1 - \xi^y) - \frac{(\sigma_{zx})_F + \Gamma_{zx}}{\rho_F \Delta z^{-}} \xi^x (1 - \xi^y)$$

$$- \frac{(\sigma_{zx})_G + \Gamma_{zx}}{\rho_G \Delta z^{-}} \xi^x \xi^y - \frac{(\sigma_{zx})_H + \Gamma_{zx}}{\rho_H \Delta z^{-}} (1 - \xi^x)\xi^y + fx^{-}$$

$$YACC^{+} = \frac{(\sigma_{xy})_{AB}}{(\rho_A \Delta x^{+} + \rho_B \Delta x^{-})} (1 - \xi^y) + \frac{(\sigma_{xy})_{DC}}{(\rho_D \Delta x^{+} + \rho_C \Delta x^{-})} \xi^y$$

$$+ \frac{(\sigma_{yy})_{AD}}{(\rho_A \Delta y^{+} + \rho_D \Delta y^{-})} (1 - \xi^x) + \frac{(\sigma_{yy})_{BC}}{(\rho_B \Delta y^{+} + \rho_C \Delta y^{-})} \xi^x$$

$$+ \frac{\left[(\sigma_{zy})_A + \Gamma_{zy}\right]}{\rho_A \Delta z^{+}} (1 - \xi^x)(1 - \xi^y) + \frac{\left[(\sigma_{zy})_B + \Gamma_{zy}\right]}{\rho_B \Delta z^{+}} \xi^x (1 - \xi^y)$$

$$+ \frac{\left[(\sigma_{zy})_C + \Gamma_{zy}\right]}{\rho_C \Delta z^{+}} \xi^x \xi^y + \frac{\left[(\sigma_{zy})_D + \Gamma_{zy}\right]}{\rho_D \Delta z^{+}} (1 - \xi^x)\xi^y + fy^{+}$$

$$YACC^{-} = \frac{(\sigma_{xy})_{EF}}{(\rho_E \Delta x^{+} + \rho_F \Delta y^{-})} (1 - \xi^y) + \frac{(\sigma_{xy})_{HG}}{(\rho_H \Delta x^{+} + \rho_G \Delta x^{-})} \xi^y$$

$$+ \frac{(\sigma_{yy})_{EH}}{(\rho_E \Delta y^{+} + \rho_H \Delta y^{-})} (1 - \xi^x) + \frac{(\sigma_{yy})_{FG}}{(\rho_F \Delta y^{+} + \rho_G \Delta y^{-})} \xi^x$$

$$- \frac{\left[(\sigma_{zy})_E + \Gamma_{zy}\right]}{\rho_E \Delta z^{-}} (1 - \xi^x)(1 - \xi^y) - \frac{\left[(\sigma_{zy})_F + \Gamma_{zy}\right]}{\rho_F \Delta z^{-}} \xi^x (1 - \xi^y)$$

$$- \frac{\left[(\sigma_{zy})_G + \Gamma_{zy}\right]}{\rho_G \Delta z^{-}} \xi^x \xi^y - \frac{\left[(\sigma_{zy})_H + \Gamma_{zy}\right]}{\rho_H \Delta z^{-}} (1 - \xi^x)\xi^y + fy^{-}$$

The damping terms fy^{+}, fy^{-}, fx^{+} and fx^{-} are

$$fx^{+} = (fx_1^{A^{+}} + fx_2^{A^{+}} + fx_3^{A^{+}}) (1 - \xi^x) (1 - \xi^y)$$

$$- (fx_1^{B^{+}} + fx_2^{B^{+}} - fx_3^{B^{+}}) \xi^x (1 - \xi^y)$$

$$+ (fx_1^{C^{+}} - fx_2^{C^{+}} - fx_3^{C^{+}}) \xi^x \xi^y$$

$$- (fx_1^{D^{+}} - fx_2^{D^{+}} + fx_3^{D^{+}}) (1 - \xi^x) \xi^y$$

$$fx^- = (fx_1^{A^-} - fx_2^{E^-} - fx_3^{E^-})\ (1 - \xi^x)\ (1 - \xi^y)$$

$$- (fx_1^{B^-} - fx_2^{F^-} + fx_3^{F^-})\ \xi^x\ (1 - \xi^y)$$

$$+ (fx_1^{C^-} + fx_2^{G^-} + fx_3^{G^-})\ \xi^x\ \xi^y$$

$$- (fx_1^{D^-} + fx_2^{H^-} - fx_3^{H^-})\ (1 - \xi^x)\ \xi^y$$

$$fy^+ = (fy_1^{A^+} + fy_2^{A^+} + fy_3^{A^+})\ (1 - \xi^x)\ (1 - \xi^y)$$

$$- (fy_1^{B^+} + fy_2^{B^+} - fy_3^{B^+})\ \xi^x\ (1 - \xi^y)$$

$$+ (fy_1^{C^+} - fy_2^{C^+} - fy_3^{C^+})\ \xi^x\ \xi^y$$

$$- (fy_1^{D^+} - fy_2^{D^+} + fy_3^{D^+})\ (1 - \xi^x)\xi^y$$

$$fy^- = (fy_1^{A^-} - fy_2^{E^-} - fy_3^{E^-})\ (1 - \xi^x)\ (1 - \xi^y)$$

$$- (fy_1^{B^-} - fy_2^{F^-} + fy_3^{F^-})\ \xi^x\ (1 - \xi^y)$$

$$+ (fy_1^{C^-} + fy_2^{G^-} + fy_3^{G^-})\ \xi^x\ \xi^y$$

$$- (fy_1^{D^-} + fy_2^{H^-} - fy_3^{H^-})\ (1 - \xi^x)\xi^y\ ,$$

where the $f\overset{A^{\pm}}{x_i}$, $f\overset{B^{\pm}}{x_i}$, etc., are calculated from Equations (7.17) through (7.19) of the TRES User's Manual, using the velocity $\dot{u}$ on the $\pm$ side of the fault. The $f\overset{A^{\pm}}{y_i}$, $f\overset{B^{\pm}}{y_i}$, etc., are calculated from analogous equations using the velocity $\dot{v}$ on the $\pm$ side of the fault.

Next, define A^+, A^-, and A:

$$A^+ = \frac{(1 - \xi^x)(1 - \xi^y)}{\rho_A \Delta z^+} + \frac{\xi^x (1 - \xi^y)}{\rho_B \Delta z^+} + \frac{\xi^x \xi^y}{\rho_C \Delta z^+} + \frac{(1 - \xi^x)\xi^y}{\rho_D \Delta z^+}$$

$$A^- = -\frac{(1 - \xi^x)(1 - \xi^y)}{\rho_E \Delta z^-} - \frac{\xi^x (1 - \xi^y)}{\rho_F \Delta z^-} - \frac{\xi^x \xi^y}{\rho_G \Delta z^-} - \frac{(1 - \xi^x)\xi^y}{\rho_H \Delta z^-}$$

$$A = 0.5 (A^+ - A^-)$$

On the slip plane, we make the following definition.

$$XSTART = 0.5 (XACC^+ - XACC^-)$$

$$YSTART = 0.5 (YACC^+ - YACC^-)$$

$$\bar{u} \equiv 0.5 (u^+ + u^-)$$

$$u' \equiv 0.5 (u^+ - u^-)$$

with similar definition for $\dot{\bar{u}}$, $\dot{u}'$, $\bar{v}$, v', $\dot{\bar{v}}$, $\dot{v}$.

The following input parameters are required for the rupture model: SFRAC, SMAX, SMIN, RUPVX, RUPVY, RCRIT.

Then, at each node on the slip surface, at time TTIME, we determine the nodal quantities, SIGXZS, SIGYZS, YZBFR, YZSTAR, ISL according to the following algorithm:

$$D = \min\left\{ \frac{[(u')^2 + (v')^2]^{1/2}}{SFRAC} , 1.0 \right\}$$

```
STRF  = (1.0 - D)*SMAX + D*SMIN

IF (ISLIP . EQ . 1 . OR . ISLIP . EQ . 3)  THEN

        U̇'  =  0.
    XSTART  =  0.

END IF

IF (ISLIP . EQ . 2 . OR . ISLIP . EQ . 3) THEN

        V̇'  =  0 .
    YSTART  =  0 .

END IF

    X  =  (J-JFOCUS) δx
    Y  =  (K-KFOCUS) δy

   TR  =  (X**2/RUPVX**2 + y**2/RUPV**2)**1/2
```

$$\dot{s} = \begin{cases} [(\dot{u}')^2 + (\dot{v}')^2]^{1/2} & \text{if } [(\dot{u}')^2 + (\dot{v}')^2] > 0 \\ (XSTART^2 + YSTART^2)^{1/2} & \text{if } [(\dot{u}')^2 + (\dot{v}')^2] = 0 \end{cases}$$

$$GX = \begin{cases} \dot{u}'/\dot{s} & \text{if } [(\dot{u}')^2 + (\dot{v}')^2] > 0 \\ XSTART/\dot{s} & \text{if } [(\dot{u}')^2 + (\dot{v}')^2] = 0 \end{cases}$$

$$GY = \begin{cases} \dot{v}'/s & \text{if } [(\dot{u}')^2 + (\dot{v}')^2] > 0 \\ YSTART/\dot{s} & \text{if } [(\dot{u}')^2 + (\dot{v}')^2] = 0 \end{cases}$$

$$YZBFR = (XSTART^2 + YSTART^2)^{1/2}/A$$

$$ISL = 1$$

If (TR . GT . TTIME . OR . R . GT . RCRIT) go to 10

$$F = \min [(TTIME-TR)/(10. * \delta t), 1.0]$$

$$STRF2 = (1. - F)*YZBFR + F*SMIN$$

If (STRF2.LT.STRF) STRF = STRF2

$$ISL = 2$$

10 $$B = .5* \delta t*STRF*A$$

$$CX = \dot{u}' + \delta t*XSTART - GX*B$$

$$CY = \dot{v}' + \delta t*YSTART - GY*B$$

$$C = (CX^2 + CY^2)^{1/2}$$

$$CX = CX/C$$

$$CY = CY/C$$

If (c · GT · B) go to 20

$$YZSTAR = [(\dot{v}'/\delta t + YSTART)^2 + (\dot{u}'/\delta t + XSTART)^2]^{1/2}/A$$

$$ISL = -ISL$$

SIGXZS = ($\dot{u}^-/\delta t$ + XSTART)/A

SIGYZS = ($\dot{v}^-/\delta t$ + YSTART)/A

Go to 220

20 YZSTAR = .5*STRF*$[(GX + CX)^2 + (GY + CY)^2]^{1/2}$

SIGXZS = .5*STRF*(GX + CX)

SIGYZS = .5*STRF*(GY + CY)

220 continue

Finally, we form the mean and differential accelerations. The differential accelerations are determined by

$$\ddot{u}^- = XSTART - A * SIGXZS$$

$$\ddot{v}^- = YSTART - A * SIGYZS,$$

and the mean accelerations are

$$\ddot{\bar{u}} = .5(XACC^+ + XACC^-) + .5(A^+ + A^-)*SIGXZS$$

$$\ddot{\bar{v}} = .5(YACC^+ + YACC^-) + .5(A^+ + A^-)*SIGYZS \quad .$$

Then

$$\ddot{u}^+ = \ddot{\bar{u}} + \ddot{u}^-$$

$$\ddot{u}^- = \ddot{\bar{u}} - \ddot{u}^-$$

$$\ddot{v}^+ = \ddot{\bar{v}} + \ddot{v}^-$$

$$\ddot{v}^- = \ddot{\bar{v}} - \ddot{v}^-$$

which can be integrated to get updated velocities $\dot{u}^+$, $\dot{u}^-$, $\dot{v}^+$, $\dot{v}^-$.